VOLUME 22, 1960/61, No. 5 pp. 141-180 Published 6 th March 1961

Philips Technical Review

DEALING WITH TECHNICAL PROBLEMS
RELATING TO THE PRODUCTS, PROCESSES AND INVESTIGATIONS OF
THE PHILIPS INDUSTRIES

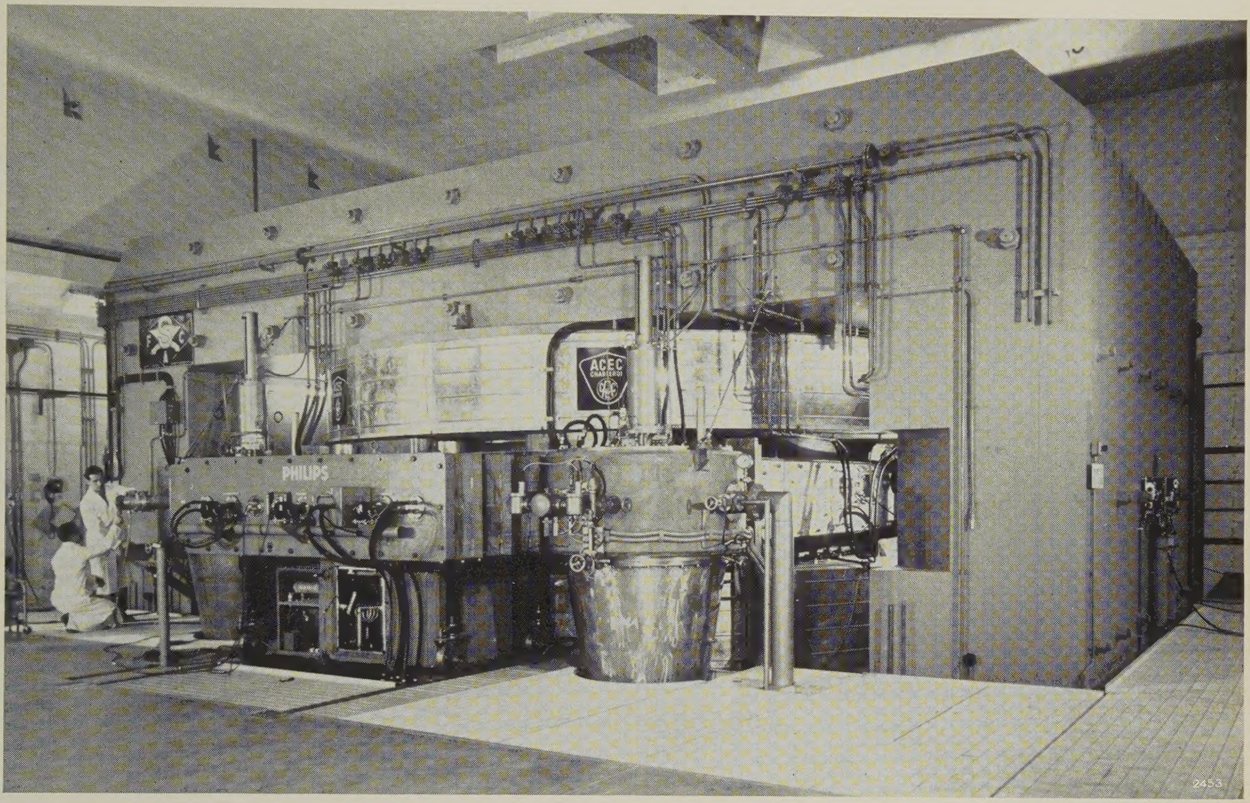

Photo CERN

THE CERN 600 MeV SYNCHROCYCLOTRON AT GENEVA

I. OBJECT AND DESIGN.
II. THE RADIO-FREQUENCY SYSTEM.
III. THE TUNING-FORK MODULATOR.

On 1st August 1957 the synchrocyclotron of the Organisation Européenne pour la Recherche Nucléaire (CERN) in Geneva entered into operation for the first time at maximum particle energy. The machine delivers protons with an energy of 600 million electron-volts, which makes it the third largest of its kind in the world (the largest is in Berkeley, California, and delivers proton energies of 740 MeV). Several European firms have contributed to the construction of the CERN cyclotron: the 2500-ton magnet was supplied by Schneider (Le Creusot, France); the energizing coils for the magnet by ACEC (Belgium); the vacuum chamber, in which the particles are accelerated by the radio-frequency field, was made by Avesta (Sweden); the large vacuum pumps for this chamber came from Leybold (Germany); etc. The entire radio-frequency system, with its modulator, was developed and manufactured by Philips Eindhoven in collaboration with the CERN.

It will be known that the principle of the cyclotron in its original form, i.e. with an accelerating voltage of constant frequency, can be used only up to relatively low values of particle energy (some tens of MeV), since the particles spiralling in the magnetic field fall out of phase with the voltage as a result of the relativistic increase in their mass. Higher energies can be achieved by frequency-modulating the RF voltage: if the frequency, during a part of the modulation period, is decreased in correspondence with the increase in mass, the particles can be kept in phase with the voltage up to the edge of the magnetic field. In this way, owing the to "phase focusing", not only the particles that have *originated at one given instant are accelerated but a whole group of particles that have originated both before and after this instant (principle of the synchrocyclotron) *).*

In most synchrocyclotrons built hitherto the accelerating voltage is frequency-modulated with the aid of a rotating capacitor. A different system was adopted for the CERN machine, a vibrating capacitor being used in the form of a giant tuning fork. A description of this new modulator system is given here. The description is prefaced by an article dealing with the general object and principal design data of the synchrocyclotron, and by a brief account of the complete radio-frequency system.

The entire installation was built under the direction of Professor W. Gentner, the plans having been drawn up mainly under the direction of Professor C. J. Bakker, afterwards Director General of the CERN, whose death in April 1960 as the result of an air crash was such a tragic loss. This series of articles was planned with the kind help of the late Professor Bakker. We are indebted to Professor Gentner for the introductory article.

I. OBJECT AND DESIGN

by W. GENTNER **).

621.384.611.2

History

Serious discussions concerning the foundation of a European laboratory for studying the physics of energetic particles were begun in 1951. At the first meeting of the provisional Conseil Européen pour la Recherche Nucléaire (CERN), agreement was reached on the general objectives, which were subsequently laid down in the Charter of the Organisation Européenne pour la Recherche Nucléaire, established in 1954. The laboratory was to be equipped with two large accelerators, on a scale not then existing in Europe. The first machine envisaged was a large synchrocyclotron, whose construction was to be based on installations of the same type and comparable energy as already proved elsewhere. The second machine was to be a pioneering project, both in regard to its particle energy (above 10 000 MeV) and its construction ¹).

Principles of the design

We shall here describe the first, smaller accelerator — later commonly referred to as the SC machine. The main object was to provide the CERN laboratory in the shortest possible time with a powerful source of pi and mu mesons, so as to enable the laboratory to play a full part in meson research. For this purpose the energy of the accelerator had to be substantially higher than the threshold value for meson production, which is about 180 MeV when protons are used, for it was already known that the production of pi mesons does not initially rise very steeply as a function of proton energy (*fig. 1*). Moreover, it was important that the mesons produced should have the widest possible energy spectrum with a view, for example, to experiments on the scattering of mesons in matter as a function of their velocity. An upper limit was set to the choice of energy by the steeply rising costs involved, and also by purely technical considerations. Like the classic

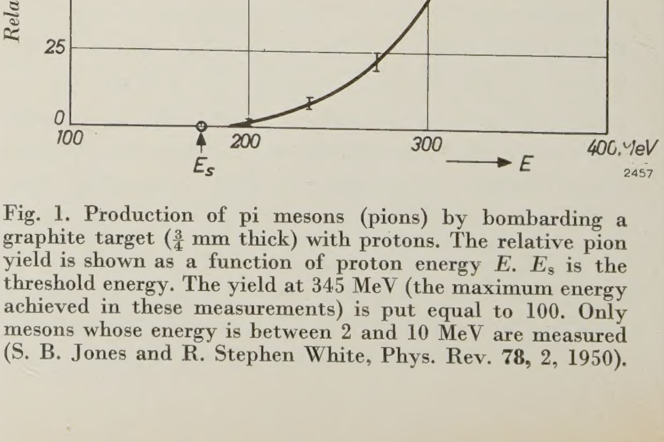

Fig. 1. Production of pi mesons (pions) by bombarding a graphite target ($\frac{3}{4}$ mm thick) with protons. The relative pion yield is shown as a function of proton energy E. E_s is the threshold energy. The yield at 345 MeV (the maximum energy achieved in these measurements) is put equal to 100. Only mesons whose energy is between 2 and 10 MeV are measured (S. B. Jones and R. Stephen White, Phys. Rev. **78**, 2, 1950).

---

*) For further details of this principle, see W. de Groot, Cyclotron and synchrocyclotron, Philips tech. Rev. **12**, 65-72, 1950/51. Fundamental problems involved in the construction of a synchrocyclotron are dealt with in the following series of articles: F. A. Heyn, The synchrocyclotron at Amsterdam, I. General description of the installation, II. The oscillator and the modulator, III. The electromagnet, IV. (with J. J. Burgerjon) Details of construction and ancillary equipment, Philips tech. Rev. **12**, 241-247, 247-256, 349-364, 1950/51, and **14**, 263-279, 1952/53.

**) Director of Max Planck Institut für Kernphysik, Heidelberg. Director of the Synchrocyclotron department of the CERN, Geneva, from 1955 to 1959.

¹) This accelerator has been completed and was officially put into operation on 5th February 1960. The proton energy achieved is 28 500 million electronvolts (28.5 GeV).

cyclotron, the synchrocyclotron requires a constant magnetic field in which the circular accelerating chamber is placed. The size of the pole pieces of the magnet was to be such as to allow them to be made on the largest available lathes in Europe. Furthermore, the pole pieces and also the energizing coils were to be transported by road. All these physical, technical and financial considerations led finally to a pole diameter of about 5 metres (cf. *fig. 2*). With a field of suitable form, it is possible with this size of magnet of obtain a maximum beam radius of 2.27 m, which, in the case of protons and with an induction at the centre of 1.9 Wb/m^2 (19 000 gauss), corresponds to an energy of approximately 600 MeV. This energy was regarded as sufficient for pi and mu meson research, particularly if high beam currents can be achieved, which was a further feature of the design. Further, the intention was not only to produce mesons on targets inside the cyclotron, but also to extract a large fraction of the internal beam of particles, in order to generate mesons on external targets.

The design of the installation was carried out by a team of engineers and physicists, largely drawn from nuclear research laboratories in the twelve member countries [2]). Numerous specialists and designers in the field of particle accelerators acted as advisers in the early years to the permanent team, which has since been steadily expanded. Finally, tenders were invited from European firms for the manufacture of the cyclotron components and ancillary equipment, orders being placed with those firms whose tenders were most satisfactory. The entire project was thus a striking example of the European cooperation which CERN set out to achieve.

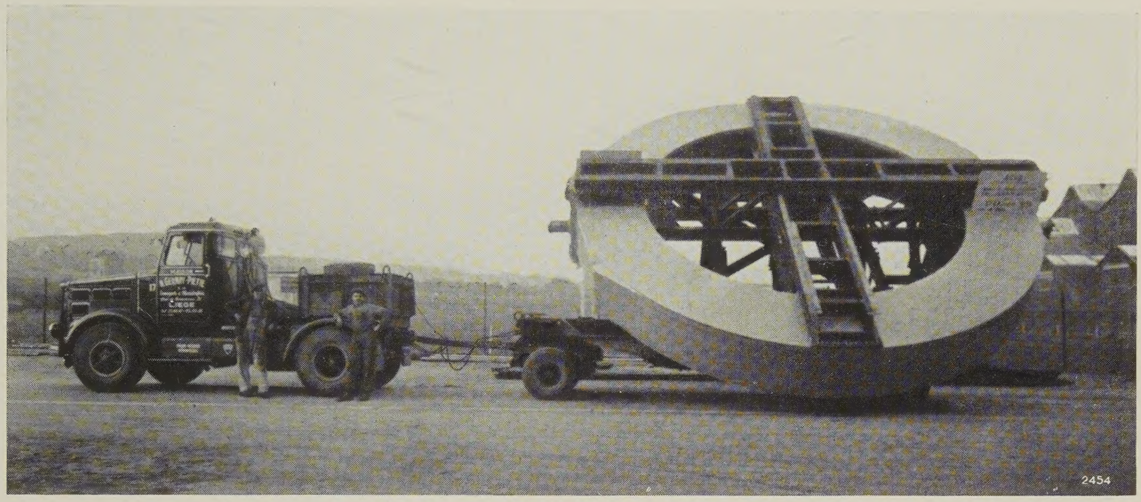

Photo CERN

Fig. 2. One of the two energizing coils (made by ACEC, Belgium) on the way to Geneva by road. The internal diameter (i.e. the pole diameter of the magnet) is roughly 5 metres.

General layout

The layout of the synchrocyclotron and the experiment rooms and beam channels can be seen in *fig. 3*. The cyclotron is situated centrally in the building, and is surrounded by a radiation shield of barium-concrete walls 6 metres thick (the barium content increases the absorption). Diametrically opposite each other, left and right in the figure, are the two rooms for experiments: left, in P, the protons are available, and right, in N, the neutrons and mesons produced inside the cyclotron. The protective partitions between the rooms and the cyclotron are built up from movable blocks, and can be made to sink into the floor, thus greatly facilitating the setting-up of new experimental arrangements. When irradiation is in progress in one of the rooms, independent experiments can be prepared in the other one. Room N, with its wall B_2, is built as close as possible to the cyclotron, since the mesons are so short-lived that they have already considerably decayed on their way to the experiment bay.

---

[2]) The member countries of CERN are Belgium, Denmark, Federal Germany, France, Great Britain, Greece, Italy, Jugoslavia, The Netherlands, Norway, Sweden and Switzerland. Austria has also been a member since 1959.

About 30 metres from the source, high earth walls provide extra protection for the other parts of the SC department. Any excessive radiation in particular directions is absorbed by concrete blocks mounted at suitable locations within the area (*fig. 4*).

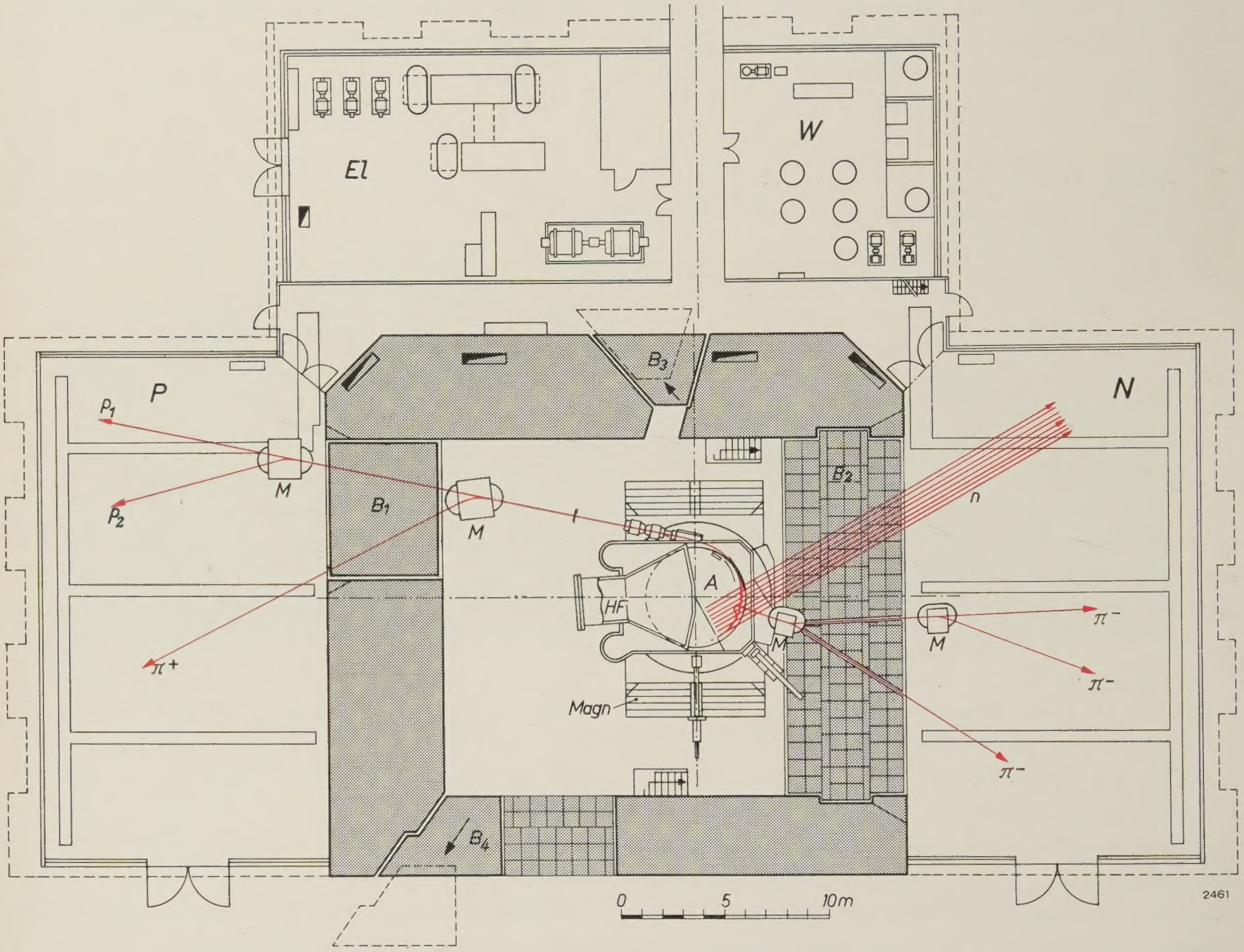

Fig. 3. Layout of the CERN synchrocyclotron, showing the concrete protective walls (shaded), the beam channels and experiment rooms (*P* for protons, *N* for neutrons). All particle beams are drawn in red: p_1 proton beam, p_2 extracted proton beam, *n* series of neutron beams generated at different radii of the proton path in the accelerating chamber *A*, π^+ and π^- beams of the positive and negative pions, respectively, extracted by suitable means and focused by magnets *M*. *Magn* cyclotron magnet. *HF* radio-frequency system. B_1 and B_2 protective partitions built up from separate concrete blocks and capable of being sunk into the floor and raised hydraulically. B_3 and B_4 concrete blocks acting as doors, movable by means of electric motors. *El* power house containing the energizing-current generators and other ancillary electrical apparatus. *W* pump house supplying the cooling water and containing the cooling installation.

A passage 60 m long leads from the cyclotron and the experiment rooms to the control room (*fig. 5*) and the "counter rooms", which contain the equipment for counting the particles in the experiments (most experiments boil down to counting operations). It is here that the cyclotron and the experiments are controlled, since it is not as a rule permissible for anyone to be in the cyclotron building when irradiations are in progress in both experiment rooms.

The fact that the cyclotron is set up at ground level — and not, as many similar installations are, underground — has the great advantage that the outside walls of the experiment rooms proper may be thin. As a result, there is very little back scatter of the radiation used in the experiments. This in no way detracts from the effectiveness of the external protection, and has proved to be of great practical value. No other comparable installation has such a low background of scattered radiation in the experiment rooms. Indeed, in many experiments this fact is of decisive importance. The thin walls offer the further

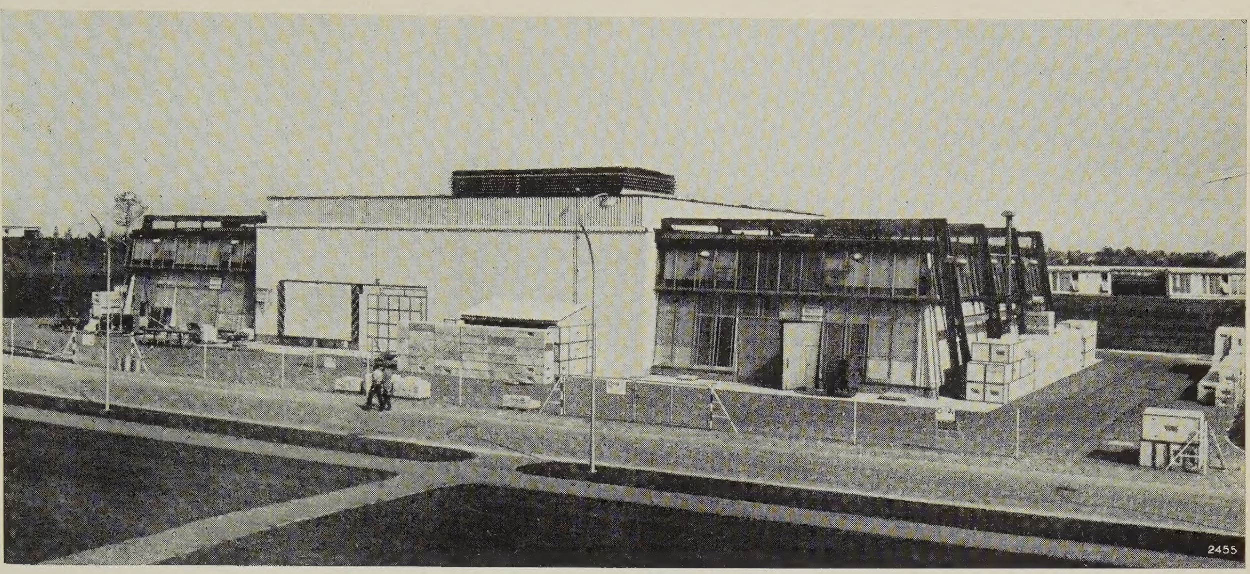

Photo CERN

Fig. 4. The building which houses the synchrocyclotron. The experiment rooms, seen right and left, in which remotely controlled instruments are subjected to bombardment by high-energy particles when the cyclotron is in operation, are enclosed by thin walls with the object of reducing back-scatter. Special directions in which radiation might penetrate outside the rooms are shielded off at some distance by concrete blocks.

advantage of making it easily possible to extend the beam channel outside if the experiments should make this necessary.

Main components

The construction of the magnet was first studied on a 1 : 10 scale model. (This model is now being used in a small cyclotron for further investigation of the acceleration process.) The magnet consists of 54 blocks, most of them weighing 46 tons each. The total weight of 2500 tons calls for a very reliable foundation. The distance between the

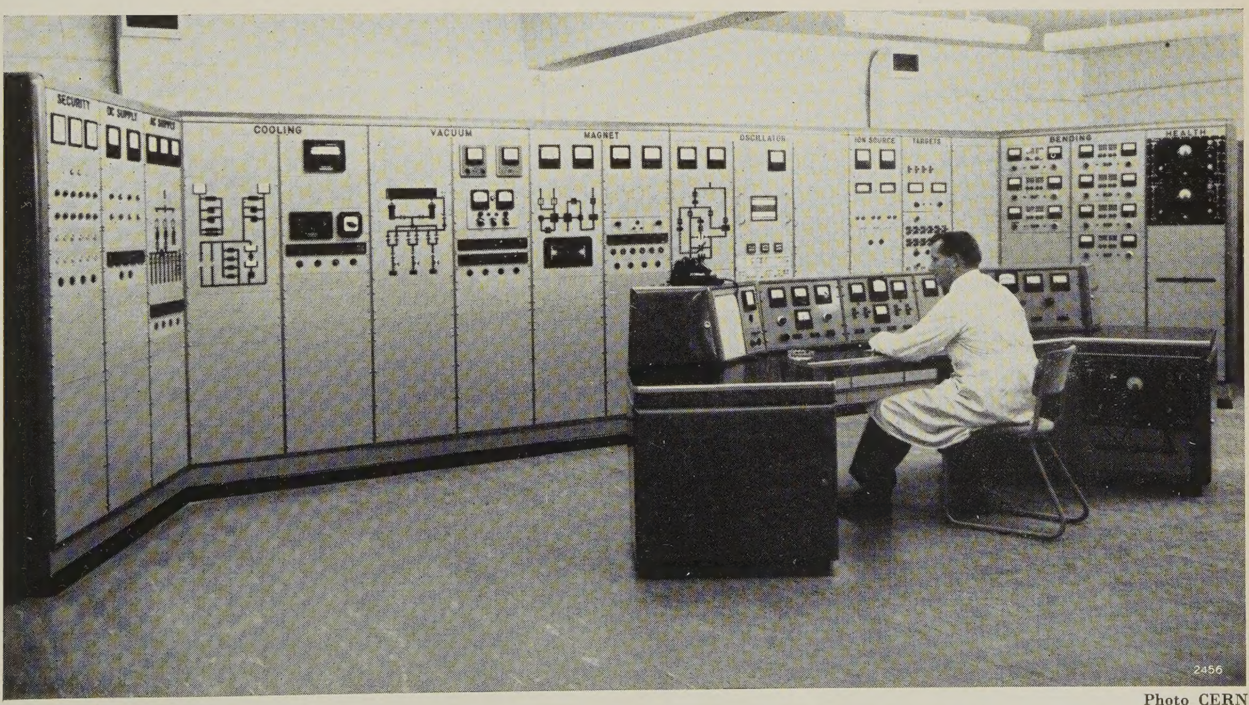

Photo CERN

Fig. 5. The master control room of the CERN synchrocyclotron.

poles varies between 45 and 35 cm. The two energizing coils are wound with aluminium tubing of rectangular cross-section, through which cooling water flows. The coils are ordinarily fed with a current of 1750 A, giving the magnetic induction at the centre of 1.9 Wb/m² mentioned above. *Fig. 6* shows the magnetic induction in the median plane between the pole pieces as a function of the radius.

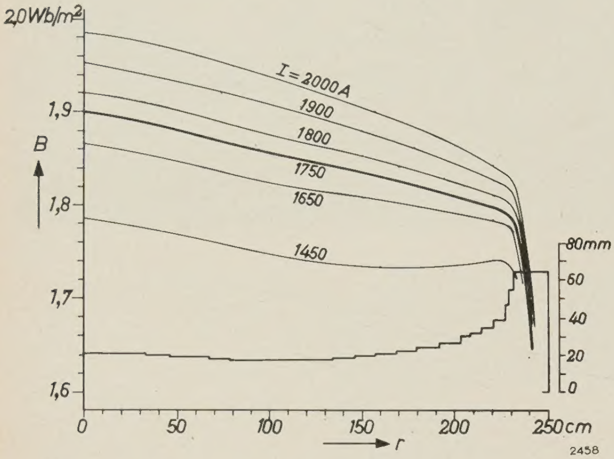

Fig. 6. Induction B in the plane midway between the poles of the magnet, as a function of the radius r, for different currents I in the energizing coils. The field shape in a synchrocyclotron is adjusted by means of ring-shaped shims of soft iron, increasing stepwise in thickness towards the edge, so as to keep the orbits of the particles stable up to the edge. The critical point where stabilization fails (i.e. where the gradient $n = (\mathrm{d}B/\mathrm{d}r)\,(r/B)$ reaches the value 0.2) lies here at the radius $r = 2.27$ metres.

The profile of the pole pieces produced by the shims is shown below the curves; see scale on right.

At a current of 1750 A the power converted into heat in the coils is approximately 750 kW. The cooling water which removes this heat is itself cooled, and is recirculated. In the title photo the upper part of the magnet can be seen, with the upper energizing coil and the accelerating chamber.

The vacuum in the accelerating chamber, which must be of the order of 10^{-6} mm Hg, is maintained by two oil-diffusion pumps, each with a pumping rate of 12 m³/sec at 10^{-4} mm Hg. The whole chamber, including the connections to the pumps, is made of stainless-steel plates welded to a frame assembly. No trouble has ever been experienced with the vacuum.

The proton source originally envisaged was a hot-cathode arc ion source. This was later replaced by a Penning cold-cathode ion source, which is much simpler and can also be pulsed without difficulty.

The radio-frequency system, on whose reliability the operation of the whole cyclotron depends, is described at some length in the following articles. The principle of the tuning fork, chosen as the variable capacitance of the modulator, providing a frequency variation between 29 and 16.5 Mc/s, finally proved its value after a good deal of difficult development work. The protons are accelerated in the RF field in the established way with only one complete Dee, which leaves one half of the acceleration chamber entirely free for the positioning of targets. The general construction of the dee and further particulars of the accelerating chamber are shown in *fig. 7*.

The machine is provided with the following target systems. For the production of neutrons of different energy, eight "flip targets" (see below, fig. 7) can be "flipped" into the beam at varying distances from the centre. A movable "probe target" can also be positioned at a varying distance from the centre; the use to which it is put will be discussed presently. Further, there is a universal target or "Fermi trolley" available, which can be moved around the outermost proton orbit and is used for the production of mesons. This system permits easy adjustment of the meson source in relation to the deflection system for the meson channels.

The proton beam is deflected in a magnetic channel in which an adjustable perturbation of the magnetic field produces suitable oscillations of the beam. This beam-extraction system, developed by Le Couteur, had already proved its effectiveness in the Liverpool synchrocyclotron [3]). Upon extraction the proton beam immediately passes through two quadrupole lenses, each of which has a focal length of about 3 m. These are followed, near the radiation shield, by a double-focusing deflection magnet, which accurately directs the beam through the channel to the experiment room.

The principal operating data of the machine are collected in *Table I.*

Yield of fast protons and mesons

The current of the internal proton beam can be measured with a thermocouple fixed to the probe target. As the radius increases, however, and with it the particle energy, the beam passes through the thermocouple more than once. At the same time,

---

[3]) K. J. Le Couteur, The extraction of the beam from the Liverpool synchrocyclotron, I. Theoretical, Proc. Roy. Soc. A **232**, 236-241, 1955. — The required magnetic channel for the CERN machine was designed with the assistance of N.F. Verster of the Philips Laboratory at Eindhoven, making use of a laboratory computer.
Editorial note: This design work, which has also been applied successfully to the synchrocyclotron built by Philips at Orsay near Paris, will in due course be the subject of a special article in this journal.

Table I. Principal data of CERN synchrocyclotron.

Maximum proton energy	600 MeV
Maximum radius R of proton path ($n = 0.2$)	2.27 m
Magnetic induction at $R = 0$, midway between the poles	1.88 Wb/m^2
Magnetic induction at $R = 2.27$ m	1.79 Wb/m^2
Ampere turns, normal	1.2×10^6
Ampere turns, maximum permissible	1.35×10^6
Energizing power, normal	750 kW
Weight of magnet	2500 tons
Frequency sweep of accelerating voltage	29-16.5 Mc/s
Modulation frequency	55 c/s

the energy loss of the particles per unit length of path is reduced. Consequently, at radii above 1.5 metres, the proportionality factor that gives the relation between the thermo-e.m.f. and the beam current is dependent on the radius. Where an absolute measurement is required, this method can therefore only be used with certain corrections, which are not so simple to estimate. For relative measurements, however, the method is most convenient. It has been shown, for example, that there is no appreciable

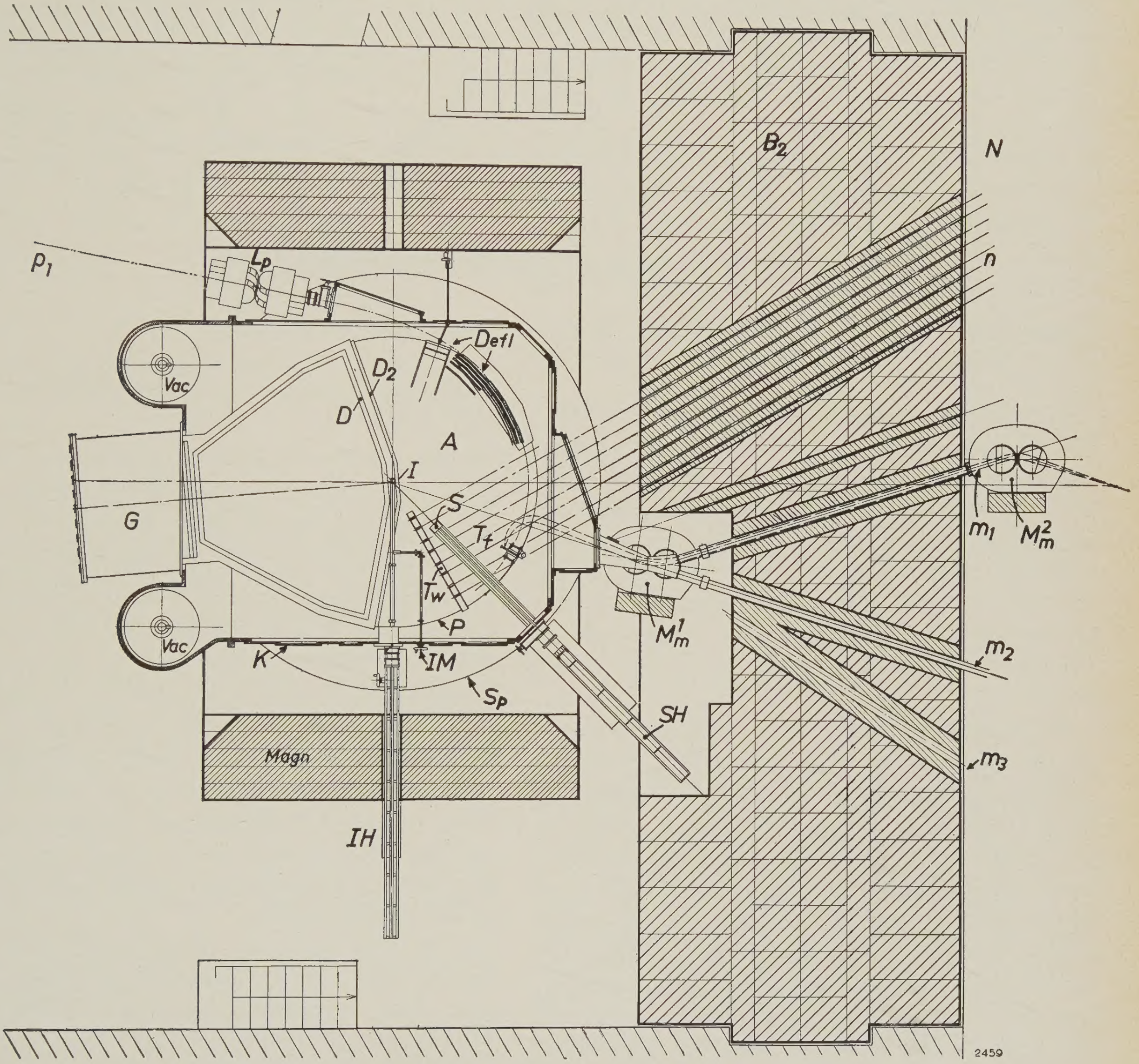

Fig. 7. The accelerating space A in the vacuum chamber K, with channels through the protective wall B_2 leading to the neutron experiment room N. Only one of the dee electrodes (D) is connected to the radio-frequency system: the second is earthed and is therefore a simple slotted strip (D_2), leaving the whole of the right half of the chamber free for target assemblies. I ion source attached to arm IH and with adjusting mechanism IM. T_w eight "flip targets", which can be set upright for producing neutrons of different energies (beams n). S probe fitted to arm SH, one purpose of which is to measure the intensity of the proton beam at various distances from the centre. *Defl* magnetic channel with devices for extracting the protons from the accelerating chamber. L_p lens for strong focusing of the extracted proton beam p_1. T_f Fermi trolley, i.e. universal target, which can be moved around the outermost proton orbit, for the production of mesons; in the position illustrated, negative pions are extracted by the deflection magnets $M_m{}^1$ and $M_m{}^2$. The meson beams are m_1, m_2, m_3. *Magn* yoke of cyclotron magnet. P magnet pole. *Sp* energizing coil. *Vac* pumps. G radio-frequency source and tuning-fork modulator.

loss of particles during the acceleration. The method was also used, with a differential thermocouple, to get the spiral paths of the protons to lie very accurately in the median plane between the pole pieces. For this purpose the energizing currents of the two large magnet coils had to be made slightly different by means of an additional current generator: the magnetic median plane was found to be originally 1.2 cm lower than the geometrical median plane.

The absolute intensity of the external beam was measured with a graphite target, in which ^{11}C is produced by the process $^{12}C(p,pn)^{11}C$. Since ^{11}C emits only positrons, the number of these reactions per unit time can easily be determined by comparing the emitted radiation with the radiation from a standard gamma source. Moreover, the effective cross-section — which gives the ratio between the number of reactions and the number of bombarding protons — is well known for this reaction, and is virtually energy-independent for protons in the energy range involved. In this way the internal proton beam current at a radius of 2 m was found to be 0.3 μA.

Extensive magnetic measurements in the deflection channel were needed in order to arrive at the highest possible intensity in the deflected beam. With the lenses referred to above, the beam in the experiment room can be focused to a diameter of 3 cm at a point 5 m beyond the radiation shield. The total external proton beam current is 1×10^{11} protons per second, i.e. about 6% of the internal current. These protons possess an energy of 600 MeV.

The experiment room at the other side receives the positive and negative pi mesons (pions) from the Fermi trolley. The energy of these pions is between 70 and 320 MeV. The negative pions describe a path as illustrated in fig. 7. The maximum intensity is reached at 150 MeV and amounts to 4×10^5 pions per sec. Since the path of the positive pions is curved in the same direction as that of the protons, only those positive pions can be extracted into an external channel that emerge from the target backwards. The Fermi trolley is moved into the appropriate position for this purpose (see *fig. 8*). Owing to this less favourable direction of emission (the majority of the pions in this energy range leave the target in the forward direction) the intensity of the positive pion beam is much lower. Other things being equal, it amounts to roughly 10^4 pions per sec at 70 MeV. It is also possible to produce pions in an external target, and to extract them from the proton beam by means of a deflection magnet (see the π^+ beam in bay *P* in fig. 3).

Results to date and future plans

After the cyclotron was first put into operation on 1st August 1957 at its maximum energy, experiments could soon begin. There was then very little time available to make the modifications which had been shown to be desirable in the first month of operation. After having worked for more than two years, the cyclotron was shut down for a while to allow these modifications to be made. Improvements were introduced in the RF system, and changes are being made that will enable the cyclotron to operate on short pulses, whilst at the time raising the intensity of the proton beam. The protective wall with the beam channels is being rebuilt, and quadrupole lenses are to be incorporated in the wall in an attempt to raise the intensity of the pion currents. Another series of quadrupole lenses is being set up to produce a powerful beam of mu mesons(muons) for scatter experiments.

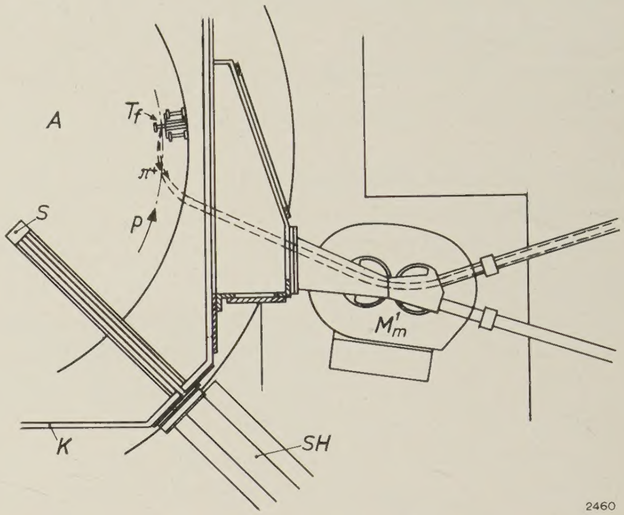

Fig. 8. Position of universal target T_f (Fermi trolley) for producing positive pions with the proton beam *p*. Meaning of letters as in fig. 7.

In the first three years the machine was in operation 24 hours a day over long periods. During this time, many interesting experiments were successfully completed. One group of investigators demonstrated that, in addition to the normal decay of the pion into a muon and a neutrino, it is also possible to observe the much rarer decay of the pion into an electron and a neutrino [4]). Other groups have worked on the K-capture of muons in ^{12}C, with the object of studying the interaction of muons and electrons with the atomic nucleus. Experiments have been carried out to test the hypothesis that meson processes are independent of their charge. A chemical team has been engaged on the study of various nuclear reactions involving the ejection of numerous fragments (spallation). In addition, guest teams from the member countries have started on their own research programmes, and these are being given special prominence.

---

[4]) F. Fazzini, G. Fidecaro, A. W. Merrison, H. Paul and A. V. Tollestrup, The electron decay of the pion, Phys. Rev. Letters 1, 247, 1958.

Summary. The synchrocyclotron of the CERN laboratory at Geneva, which has been in operation since August 1957, produces protons of 600 MeV. This article discusses briefly the principal considerations governing the choice of this energy and the general design. Of particular interest is the layout of the building, which made it possible to minimize the general background of radiation in the experiment rooms. After mentioning the salient features of the construction of the synchrocyclotron, the author touches on the targets and the beams of particles produced. The internal proton beam current is approx. 0.3 μA. An efficient deflection system makes it possible to extract about 6% of this current. Further, intensive beams of pions and muons are available (per second 4×10^5 negative pions of 150 MeV or 10^4 positive pions of 70 MeV). The article concludes with a reference to the research programmes in progress.

II. THE RADIO-FREQUENCY SYSTEM

by K. H. SCHMITTER *) and S. KORTLEVEN **).

621.384.611.2

In the following account of the radio-frequency system of the CERN synchrocyclotron we shall describe the main technical features of the system and also touch briefly on the theoretical considerations underlying its design. Some parameters on which the design is based have already been mentioned in the previous article (particle energy, magnetic induction, dimensions of the magnet poles, etc.); various other conditions were imposed by the design of the modulator, which is described in article III.

Principles underlying the design

The orbital frequency ω of the particles in a cyclotron decreases during the acceleration process, for two reasons:

1) because of the relativistic increase of the mass m of the particles,

2) because the magnetic induction B falls off radially. This radial diminution of the field in the (rotationally symmetric) cyclotron is necessary in order to stabilize the orbits of the particles. Let m_0 be the rest mass of the particles, e their charge, r the radius of the orbit and c the velocity of light, then the familiar equation applicable to the classic cyclotron,

$$\omega_0 = \frac{eB}{m_0}, \quad \ldots\ldots\ldots \quad (1)$$

should be replaced by the more general equation:

$$\omega(r) = \frac{e\,B(r)}{m_0\sqrt{1+\left(\dfrac{r\,e\,B(r)}{m_0 c}\right)^2}}. \quad \ldots \quad (2)$$

For a particle at r which possesses the kinetic energy E_k corresponding to that position, the dee voltage must have the frequency given by equation (2) if the orbiting particle is to remain exactly in phase with this voltage. Equation (2) thus gives the ideal frequency variation in an acceleration cycle, and that variation should be achieved in the synchrocyclotron by modulating the frequency of the dee voltage. *Fig. 1* shows the induction curve $B(r)$ — see article I, fig. 6 — and the proton frequency curve $\omega(r)$, together with the curve representing the kinetic energy of the protons $E_\mathrm{k}(r)$. As can be seen, the frequency $\omega/2\pi$ for protons must initially be about 29 Mc/s for a magnetic induction at the centre of 1.9 Wb/m^2, and at the energy of 600 MeV, which corresponds to the boundary radius of 2.27 m of the stable orbit (see I), this frequency must have dropped to 16.5 Mc/s.

Broadly speaking, the above shows that the frequency sweep must be greater the higher the

---

*) Max Planck Institut für Physik und Astrophysik, Munich; formerly attached to CERN, Geneva.

**) Industrial Equipment Division, Philips, Eindhoven.

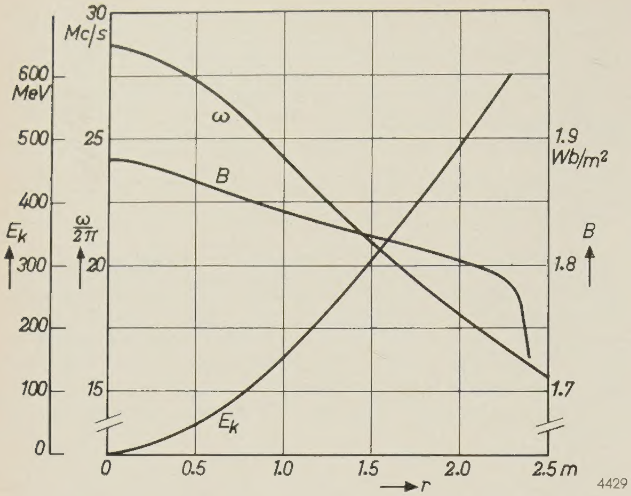

Fig. 1. Curve showing the radial variation $B(r)$ of the magnetic induction in the CERN cyclotron, the corresponding frequency variation $\omega(r)$ for the acceleration of protons, and the radial increase in the kinetic energy $E_k(r)$ of the protons.

energies aimed at 1)). That is one of the reasons why the building of a large synchrocyclotron is no easy task from the point of view of high-frequency engineering.

The above equation does not unambiguously establish the manner in which the frequency of the dee voltage should vary as a function of time between the specified limiting values. A further condition remaining to be satisfied is that the frequency variation of the particles per orbit $(\dot{\omega}/\omega)$ must exactly correspond to the energy gain of the particles in each complete orbit. For any given frequency curve one can thus derive an ideal programme for the amplitude $\hat{U}$ of the dee voltage, since the latter governs the energy gain per orbit. If we want to let the radius of the orbit increase linearly with time — in which case the curve $\omega(r)$ in fig. 1 would also represent the variation with *time* (the frequency programme) — then $\hat{U}$ = const. would be the corresponding ideal amplitude programme.

In reality the choice of amplitude and frequency programme is not entirely free, in particular because — as we shall see — the dee voltage necessarily varies with frequency. Fortunately it is not necessary that frequency and amplitude should be exactly in step with one another: if this *were* so it would mean that a particle, in each revolution, would pass the dee gap in the same phase φ with respect to the dee voltage, namely at $\varphi = -30°$. (Such particles are then 60° in phase behind those particles which pass the dee gap at the exact moment of maximum dee voltage, for which, by definition, $\varphi = -90°$.) However, because of the phase focusing, which characterizes the operation of the synchrocyclotron, a certain variation in phase is permissible; the only consequence of a deviation of φ from the chosen value is that the phase range of the particles carried along by the focusing will change slightly, thereby also changing the beam current of the cyclotron. The value $\varphi = -30°$ is generally regarded as the most favourable. It is true that at $\varphi = -90°$ the acceleration benefits from the maximum instantaneous value of the dee voltage, but the effect of the phase focusing is then zero since in that situation there is no available reserve of acceleration for the particles travelling too slowly. At $\varphi = -30°$ the focusing embraces all particles in a phase range from $-150°$ to $+40°$ 2)); only 10% of the available particles are lost and the instantaneous value of the accelerating dee voltage still amounts to half the maximum.

The practical consequence of this is that the actual amplitude of the dee voltage should always, to be on the safe side, exceed the "ideal" amplitude. True, the accompanying increase in the beam current by no means comes up to the higher demands made on the equipment to produce a higher dee voltage, but there is at least the certainty that the dee voltage will never fall *below* the ideal value, even if a dip should occur in the amplitude curve, as may happen at certain frequencies: in the latter case the beam current would fall rapidly, since many particles not accurately in phase would be lost when traversing the frequency region in which the dip appeared.

The amplitude of the dee voltage and the amplitude programme approximately establish the admissible repetition frequency of the acceleration process (modulation frequency). Given an average phase $\varphi = -30°$ and a dee voltage $\hat{U}$ of say 4 kV at 29 Mc/s and 8 kV at 16.5 Mc/s, each proton has an average energy gain of about 200 MeV per millisecond; it should thus reach the final energy of 600 MeV in about $\frac{1}{300}$th second. Since the form of the frequency curve is suitable only during roughly a third part of the modulation period, it follows that the maximum permissible value of the modulation frequency would be about 100 c/s. Unfortunately, owing to the limited mechanical strength of the material used for the mechanical modulator (see article III), it is not possible to achieve such a high

---

1) For comparison it may be mentioned that a frequency sweep of only 4% was needed in the synchrocyclotron built by Philips for the Kernfysisch Instituut (IKO) at Amsterdam, and which supplies deuterons of 28 MeV; see Philips tech. Rev. 12, 244, 1950/51.

2) D. Bohm and L. L. Foldy, Phys. Rev. **72**, 649, 1947. See also W. de Groot, Philips tech. Rev. **12**, 65, 1950/51.

modulation frequency [3]). Originally, therefore, 50 c/s was decided upon, the idea being to use the mains frequency. When it appeared, however, that the mains frequency was not sufficiently constant, it was decided to use a special generator, and the modulation frequency was fixed at 55 c/s in order to avoid beat-frequency interference from the mains.

The next step in the design of the RF system was to estimate the power required. As in most particle accelerators, the power needed for the actual acceleration is of secondary importance. The average particle current envisaged was 0.5 μA, which meant a power consumption of 300 W at a final energy of 600 MeV. Taking into account the particles lost during the acceleration process, the average RF power required for the acceleration was thus estimated at roughly 1 kW. The joule losses in the dee system, however, and other losses whose nature is not entirely clear but which generally occur in cyclotrons, are very much larger than the power needed for the actual acceleration, so that the oscillator power decided on was 10 to 20 kW [4]).

The design of the dee system

The dee system as a resonant transmission line

In a synchrocyclotron the accelerating electrodes normally consist of only one dee and an earthed strip (see I). With its supply line the dee constitutes the inner conductor of a coaxial line, which must be excited into resonance (the inner and outer conductors of the coaxial line in this case have a rectangular cross-section, and the inner conductor is hollow). Other forms of resonators are not suitable because of radiation losses. The resonator is excited in its fundamental mode. Its "electrical length" is varied by varying the boundary conditions: the modulator does this at the repetition frequency (55 c/s). The variation in the present apparatus is brought about by the variable capacitance C_M of the tuning fork.

In the simplest case, illustrated in *fig. 2*, the fundamental mode for the limiting value $C_M = 0$ (line open at both ends) corresponds to a half-wavelength along the transmission line; for the other limiting value, $C_M = \infty$ (line short-circuited at one end), it corresponds to a quarter-wavelength along the line. The corresponding resonant frequencies would be in the ratio 2 : 1. Since the practicable capacitance variation lies between much narrower limits than between 0 and ∞ — between 256 and 2580 pF with the envisaged tuning-fork modulator — it was obvious that the required frequency sweep from 29 to 16.5 Mc/s could *not* be achieved with this arrangement.

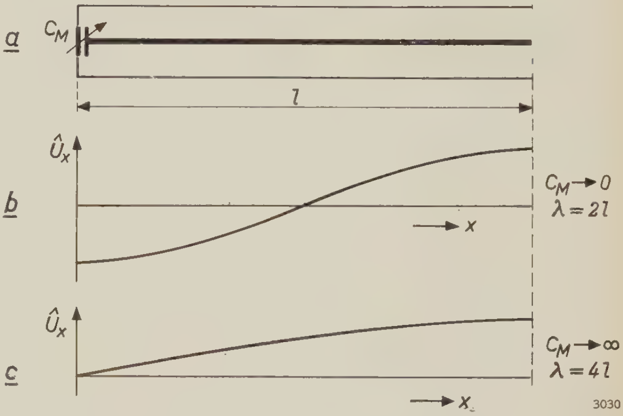

Fig. 2. *a*) Simplest form of a coaxial transmission line coupled to modulating capacitor C_M.
b) and *c*) At the limiting values $C_M = 0$ and $C_M = \infty$, a standing wave of $\frac{1}{2}\lambda$ and $\frac{1}{4}\lambda$, respectively, is set up in the resonator (the voltage amplitude $\hat{U}_x$ is plotted against distance x).

A greater frequency variation can be obtained if the modulation capacitor is made into a series resonant circuit by the addition of an inductance (*fig. 3a*) [5]). The inductance used is in the form of a shorted section of coaxial line (a "stub", fig. 3*b*). Assuming that the line has everywhere the same characteristic impedance, we then obtain the voltage distributions shown in fig. 3*c*-*g* for the limiting values $C_M = 0$ and $C_M = \infty$ and for various values in between. The whole transmission line will then have a $\frac{3}{4}\lambda$ standing wave in the one limiting case and a $\frac{1}{4}\lambda$ wave in the other, so that the extreme frequencies in the ideal case are in the ratio of 3 : 1. This brings us in sight of the desired frequency sweep (29 : 16.5), but it is evident from the cases (*d*) and (*f*) in the figure that only a frequency ratio of 5 : 3 (= 29 : 17.5) is reached at a capacitance ratio of $C_{M\max} : C_{M\min} = \pi^2 = 9.85$. We were thus still some way from our objective, and the last steps were the most difficult.

Before dealing with them, however, we shall dwell for a moment on the case of fig. 3*f*, which corresponds to the largest obtainable capacitance

---

[3]) If a rotating capacitor had been used instead of the tuning fork, the properties of the material would have imposed a similar limit on the frequency.

[4]) In the Amsterdam synchrocyclotron the "efficiency" (power on the target divided by transmitter power) is about 15%, which may be regarded as exceptionally high.

[5]) A parallel resonant circuit is also feasible, but the results are not so favourable. The intricate considerations involved are described by K. H. Schmitter, CERN report 59-33 of 22th September 1959, in which other questions concerning the resonator system are also discussed. See also M. Morpurgo, CERN report SC 136, 1955.

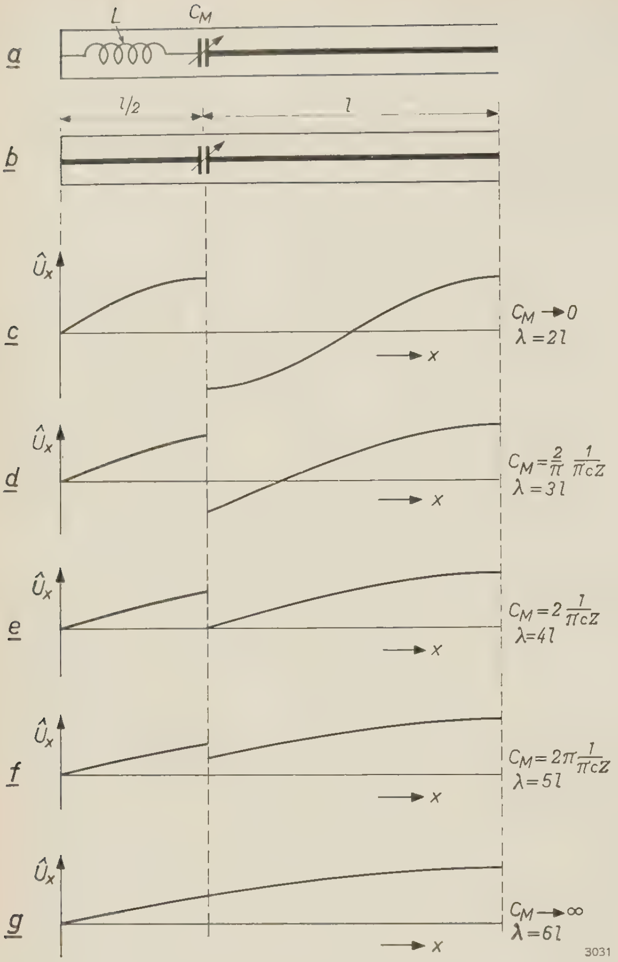

Fig. 3. *a*) The modulating capacitor is turned into a series resonant circuit by the addition of an inductance *L*.
b) This inductance is in reality a short-circuited section of line (stub).
c) to *g*) Voltage distribution on the resonator thus formed, at different values of capacitance C_M. Cases (*d*) and (*f*) roughly correspond to the extreme values attainable with the tuning-fork capacitor.

C_{Mmax}, that is to the lowest frequency. We see that in this case the resonator from the lips of the dee to the modulator must have an electrical length $l = \lambda_{\max}/5$. With $f_{\min} = 16.5$ Mc/s this gives $l = 3.75$ m. Since the length of the dee is roughly equal to the radius of the magnet pole, i.e. 2.5 m, the dee had to be provided with an extension — a stem or neck. For constructional reasons this was in fact most welcome, 1) because it created more room for the modulator (the larger a cyclotron, the more likely that the whole RF system has to be squeezed in the rather inadequate space between the coils of the large magnet), and 2) because the modulating capacitor is then situated farther away from the stray field of the magnet (see III).

The way in which the frequency sweep was finally raised to the required value may be explained by considering the influence of the characteristic impedance. To begin with, at a given variation ΔC_M of the modulator capacitance the frequency sweep will be greater the smaller is the capacitance in parallel with the modulator. It is therefore important to keep the capacitance of the dee as small as possible, that is the dee should not be larger than is absolutely necessary (half the area of the magnet poles). The characteristic impedance of the dee, which for a uniform line would be $\zeta = \sqrt{L_I/C_I}$ (L_I and C_I being respectively the inductance and capacitance per unit length), is then as large as possible. Further considerations must take into account the fact that the dee can certainly not be treated as a uniform line — this is evident on purely geometrical grounds, see the model in *fig. 4*. This at once raises the question whether the situation might not perhaps be more favourable if, also for the dee stem and stub, we were to drop the assumption hitherto made that the system is a uniform line, possessing the same characteristic impedance everywhere along it. It turns out that it is indeed better to make the characteristic impedance of the dee stem greater than that of the dee itself, and similar considerations apply to the stub, as explained in the first report cited in reference [5]). (The situation as regards the stub may be roughly understood if we remember that a large characteristic impedance implies an approach to the ideal case of a pure inductance, as in fig. 3.) Admittedly, it is not possible to take full advantage of the resultant possibilities of increasing the frequency sweep, for one reason because the latter is also limited, at a given ΔC_M, by the current and voltage load of the modu-

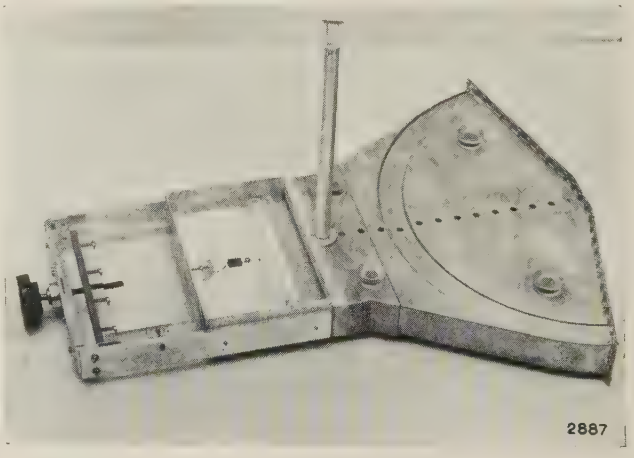

Fig. 4. Model of resonator on 1 : 10 scale. The photograph shows the outer conductor of the "coaxial" system, which, however, is removed on the left-hand side in order to show the modulating capacitor and the stub. Inside the outer conductor on the right is the dee. By means of the adjusting screw on the bracket on the extreme left the capacitance of the simulated tuning fork (meshed comb capacitor) can be changed.

lating capacitor. Nevertheless, after empirically arriving at a suitable compromise, it proved possible along these lines to achieve the required frequency sweep.

The fact that the current and voltage load affects the frequency sweep is due to the direct relation between the frequency variation at a given ΔC_M and the variation of the wattless power in the capacitor. This relation remains, no matter how the capacitor circuit may be varied; this can easily be verified on a number of simple examples.

One further remark before we enter into details on the design of the resonator. We have considered the dee system as a one-dimensional system, that is to say we have assumed that the voltage varies in the same phase and with the same amplitude at all places in the mouth of the dee. A glance at fig. 4 will make it obvious that vibration modes must also exist for which this is not the case, i.e. transverse vibrations in the dee. Such parasitic oscillations are of course unwanted. Since transversal parasitic oscillations having an antinode on the axis of symmetry are particularly likely to occur, countermeasures have been taken in some cyclotrons by cutting a slot in the dee along the axis of symmetry. Longitudinal modes are not affected by this slot. In the present case, such a measure was found to be not necessary in view of the high degree of symmetry of the system. The only dangerous parasitic oscillations were those due to the supply lines to the oscillator (these were longitudinal modes of oscillation differing from those in fig. 3). After we had adopted the principle of the flywheel oscillator, to be discussed below, even parasitic modes of this kind occasioned no further difficulties, whereas in the construction of other cyclotrons it has often taken months of hard work to eliminate the effects of parasites.

Design of the resonator

From the desired frequency programme and the variation of the tuning-fork capacitance we can now, along the lines discussed above, calculate the dimensions of a resonator as in fig. 3, provided we know the characteristic impedance of the dee. As we have seen, the dee is by no means a uniform line. Satisfactory approximation is obtained by substituting for the dee five consecutive sections of line of equal length, each in itself being a uniform line. The first section is loaded with the 200 pF capacitance of the dee mouth (*fig. 5*). We can now calculate the characteristic impedance of each section of line, and hence the reactance of the whole system as a function of frequency (*fig. 6*). Comparison of the reactance curve with that calculated when the dee is replaced by a uniform line (dashed curve in fig. 6) demonstrates the effect of the improved approximation.

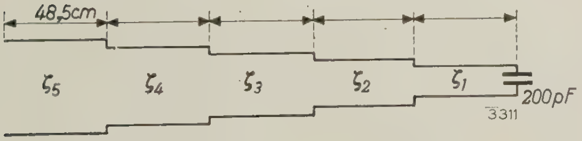

Fig. 5. Approximation to the dee by a line whose characteristic impedance ζ varies in steps, being constant in each section. The first section of line is loaded by the capacitance of the dee mouth. The steps drawn in the dee are merely a symbolic representation of the variation of ζ.

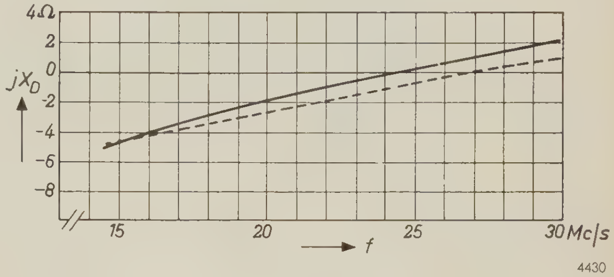

Fig. 6. Calculated reactance of the dee in fig. 5 as a function of frequency. The dashed curve represents the reactance calculated when the dee is treated as a uniform line.

The further design of the resonator was carried out, as is usual with such complicated systems, on partly empirical lines, that is the calculation outlined above was continuously supplemented and improved by a series of concurrent tests on models. One model was made on a scale of 1 : 10 (i.e. for frequencies ten times as high), and one full-scale model was made. The small model appears in fig. 4, and the full-scale model in *fig. 7*. Measurements were also made on a model of 1 : 1 scale in the longitudinal direction and 1 : 7 scale in the transverse direction. The full-scale model was also used for developing and proving the RF generator. This model — made of copper sheets on a wooden frame — was constructed in such a way as to enable the characteristic impedances of stem and stub to be varied independently of one another by changing the dimensions of the outer conductor (the "liner"). It was also possible to vary the length of the stub. In this model the tuning-fork modulator was replaced by a stationary condenser of similar shape, the capacitance of which could be varied from 250 to 2700 pF by adjusting an air gap.

The principal dimensions of the final version of the

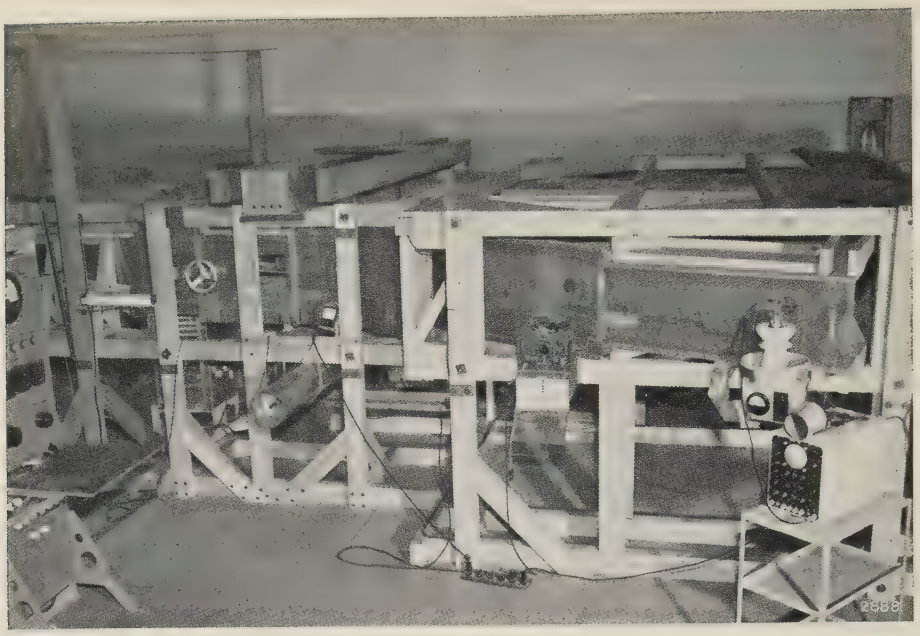

Fig. 7. Full-scale model of the resonator (wooden frame clad with sheet copper), built in Eindhoven, together with instruments for testing the RF generator.

resonator are given in *fig. 8*. The variation of the resonant frequency measured on this version as a function of the capacitance of the tuning fork is shown in *fig. 9*. For this measurement the connection terminal of the generator was placed as near as possible to the shorted end of the stub. This must be done because the capacitative reactance of the generator lowers the frequencies obtained but especially the highest frequency, the more so the farther the connection point is removed from the shorted end. This is easiest to understand if one remembers that the effect of the inductance, which was specially introduced to increase the frequency sweep (fig. 3*a*), is partly destroyed by the capacitance of the generator (primarily the anode capacitance of the transmitting valve). On the other hand, the connection terminal must not be too near the shorted end, otherwise the impedance in the anode circuit will be too small, making it impossible to satisfy the oscillation condition in the whole range of the frequency variation. The necessary minimum distance was determined empirically on the full-scale model. The dashed curve in fig. 9 represents the frequency variation calculated, taking into account the known generator reactance. *Fig. 10* shows how the frequency varies as a function of time when the tuning fork is made to vibrate sinusoidally (see III).

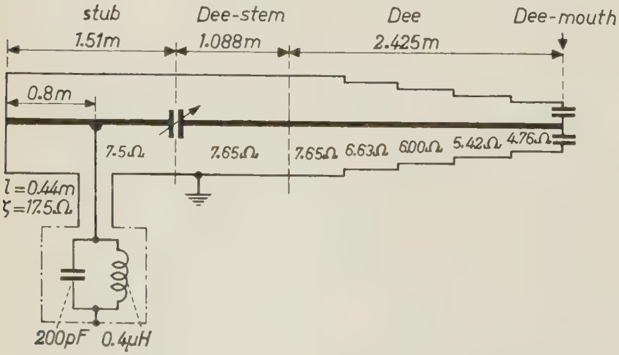

Fig. 8. Principal dimensions and characteristic impedances of the resonator in its final form.

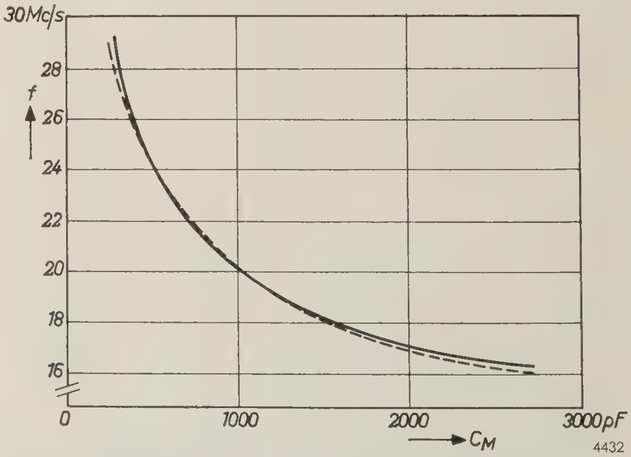

Fig. 9. Measured variation of the natural frequency f of the resonator as a function of tuning-fork capacitance C_M. The dashed curve represents the calculated variation.

Fig. 11 illustrates the voltage and current distribution over the system at the two extreme frequencies, on the assumption that the amplitude of the

RF supply voltage is constant at 5.4 kV (which corresponds to a direct anode voltage of 5 kV on the transmitting valve). It can be seen that current amplitudes of 3000 A occur in the stub, and that the voltage at the dee mouth rises from about 5 kV at 29 Mc/s to about 19 kV at 16.5 Mc/s. If we calculate the dee-voltage amplitude for the frequencies in between these values, we obtain the curve shown in *fig. 12.* This curve should be compared with the ideal amplitude programme corresponding to the frequency curve in fig. 10 if we wish to keep the phase constant at —30° (see page 150). As already explained, the deviations occurring enable the acceleration to act on the maximum number of particles, and also provide the reserve needed in the event of dips appearing in the amplitude curve of the dee voltage.

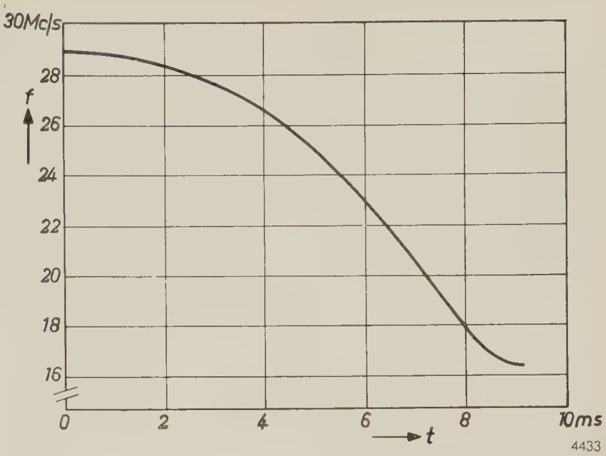

Fig. 10. Curve showing the natural frequency f of the resonator coupled to the oscillator as a function of time, for sinusoidal vibration of the tuning fork.

In reality, it is difficult to supply the system with a generator voltage of constant amplitude, owing to the effect of load variations on the excitation of the generator. In practice, therefore, the amplitude variation of the dee voltage differs from the calculated curve, as shown by the dot-dash curve in fig. 12. The curve bends over at the lowest frequencies because the generator in this region is faced with a circuit of relatively large capacitance and low inductance; such a circuit is difficult to set in oscillation, as will be seen by comparing it with the mechanical analogue of a stiff spring with a very small mass. At the higher frequencies the generator is presented with a more normal oscillatory circuit. The relatively large initial voltage which this gives rise to is very useful for drawing large numbers of ions out of the space-charge region near the axis of the cyclotron and making them take part in the acceleration process.

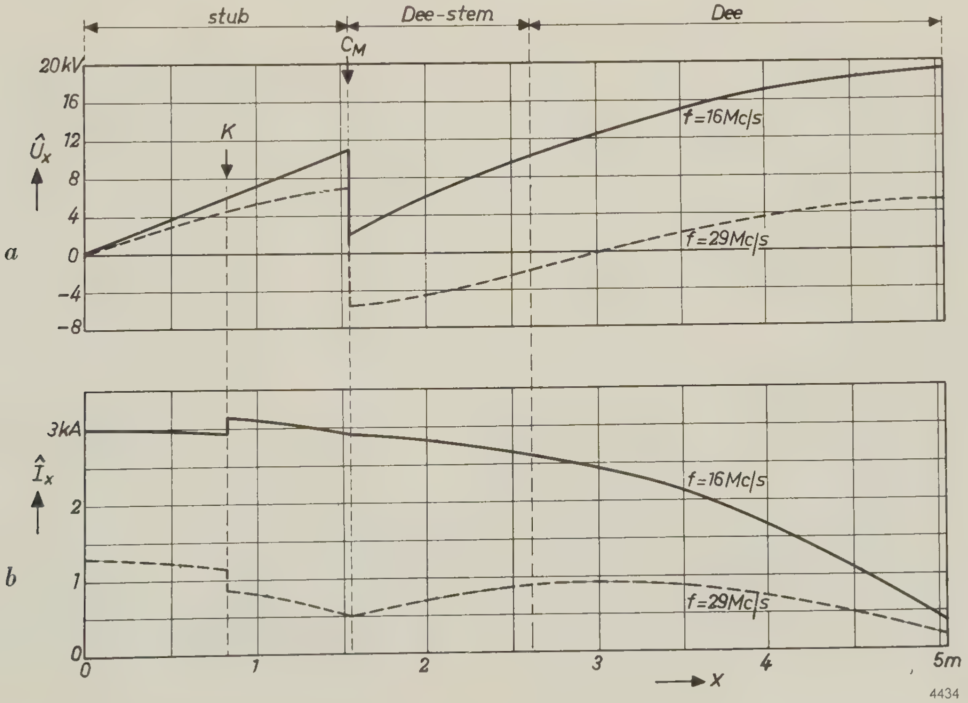

Fig. 11. *a*) Distribution of the voltage amplitude $\hat{U}$, *b*) of the current amplitude $\hat{I}$ over the resonator at the frequencies $f = 16$ Mc/s and $f = 29$ Mc/s. The abscissa x is the distance from the end of the stub. The RF voltage from the oscillator is applied at point K, it being assumed for both frequencies that the amplitude of the RF voltage on the oscillator and of the connecting line is 5.4 kV.

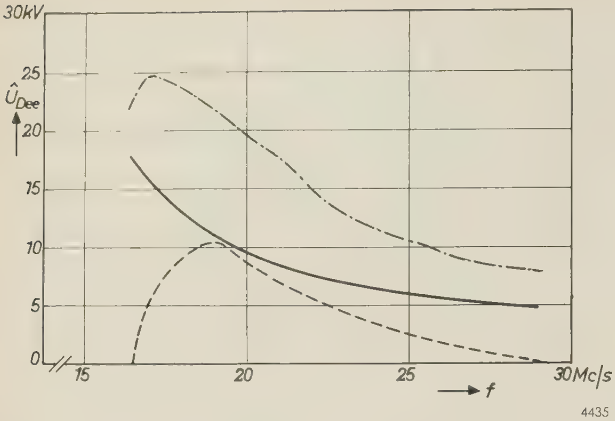

Fig. 12. Solid curve: amplitude of the voltage $\hat{U}_{\text{dee}}$ at the dee mouth, calculated as a function of frequency f. Dashed curve: the ideal amplitude programme corresponding to the frequency variation shown in fig. 10. Dot-dash curve: actual variation of voltage amplitude.

Construction of the resonator

The whole inner conductor of the resonator, consisting of dee, stem, tuning fork and stub, is under high vacuum; the stub is accommodated in an extension housing connected to the evacuated accelerating chamber of the cyclotron. *Fig. 13* shows the resonator seen from above, and *fig. 14* represents a longitudinal section. The stem H and the dee itself, D, form a single structural assembly. It is supported on two spherical insulators Is_1, at two places near the ends of the dee mouth, and at the stem it is suspended at two places by insulators Is_2. The spherical insulators rest on the lower pole plate P_2 of the magnet, which is the floor of the accelerating chamber. The insulators can roll slightly on this plate. With this mounting of dee and stem, deformations due to thermal expansion or to magnetic forces cause no significant mechanical strains in the long axis. (When the enormous magnet is switched on, the upper and lower pole plates approach each other by several millimetres!) Transverse strains are taken up by the insulators Is_2, which are specially designed for that purpose. The reinforcement ribs carried by the upper and lower plates of the dee (fig. 13) are bent upwards slightly, to compensate for the bending that occurs with the assembly supported by only two spherical insulators situated far apart. *Fig. 15* shows a photograph of the dee mounted between the pole plates; note the relatively narrow dee mouth.

The spherical insulators are surrounded by metal shields to protect them from fast particles. The dee mouth, the sides of the dee and of the stem, and the contact faces of the spherical insulators are all water-cooled. For this purpose the dee system is fitted with two parallel cooling circuits, in each of which the cooling water is supplied and returned through two hoses of hard polyvinyl chloride about 10 metres long, which insulate the system from earth. The hoses are rolled up and stored in the compartment Q. They pass through the vacuum-tight insulators Is_2 to the dee system.

Perpendicularly below the insulators Is_2 are two identical insulators Is_3; these have no supporting function but act only as insulating ports for the lines to the tuning-fork feelers X (see article III, fig. 24).

The stub St, with the tuning fork T attached to it, is suspended from two insulators Is_4, which are mounted on top of the stub housing G and are of the same construction as the Is_2 insulators. The possibility of passing lines through these insulators was not used in this case, but their construction has the advantage of allowing considerable freedom of movement in the suspension, which facilitates the initial adjustment of the tuning fork. The centre of gravity of the entire stub lies almost perpendicularly under the line joining the suspension points, so that virtually no bending moments act on the insulators. As an additional support the shorted end of the stub is secured to the floor of the housing via a simple insulator Is_5; the latter is necessary to keep this end insulated from earth for DC voltage (see below). The stub and the foot of the tuning fork (see fig. 22 in article III) are water-cooled, the supply lines passing through the rear wall of the stub housing. When the cyclotron is in operation, the entire stub housing

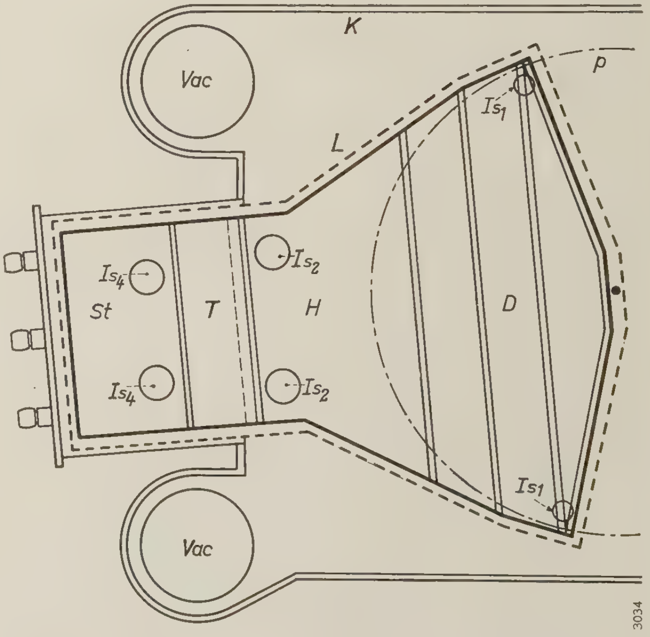

Fig. 13. Construction of the resonator and its positioning in the cyclotron. D dee with reinforcement ribs, supported at the two points Is_1. H dee stem, suspended at the two points Is_2. T tuning fork. St stub, suspended at the two points Is_4. L outer conductor of resonator. K accelerating chamber. Vac pumps. p outermost proton orbit.

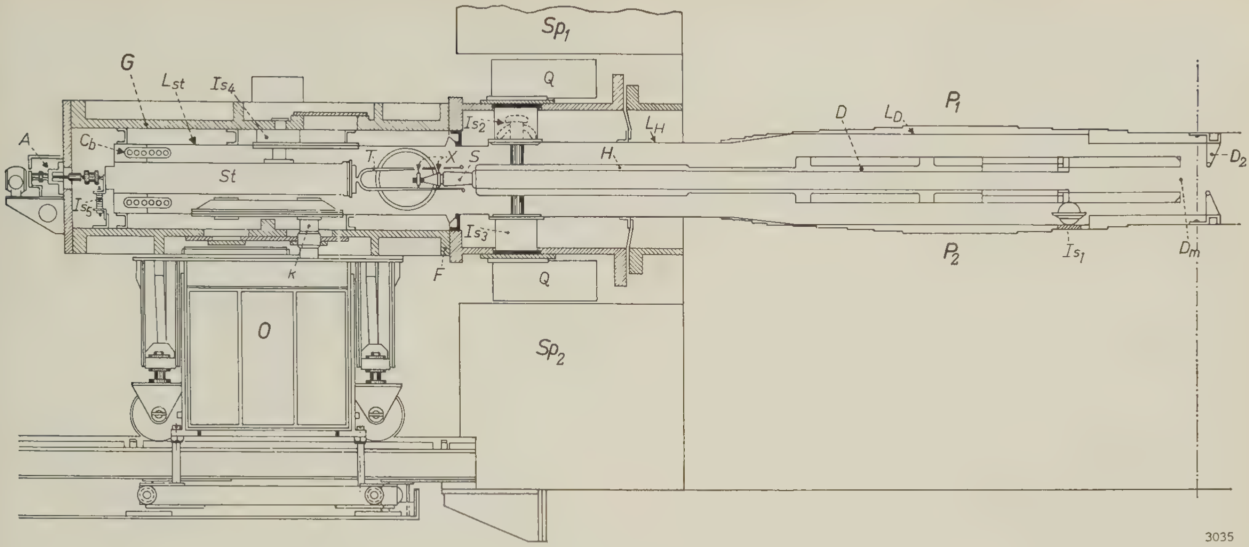

Fig. 14. Longitudinal section through the RF system. The dee *D* and dee stem *H* form an integral assembly. D_m dee mouth. D_2 dummy dee. P_1 and P_2 pole pieces of cyclotron magnet with shims, likewise ceiling and floor of accelerating chamber. Is_1 spherical insulators. Is_2 and Is_3 vacuum-tight lead-in insulators for the dee stem. *S* stator and *T* tuning fork of the modulator, with feelers *X*. *St* stub, suspended in the housing *G* from the insulators Is_4 and secured by the insulator Is_5. C_b shorting capacitor. *A* servo mechanisms for adjusting the mounting of the tuning fork. *F* flange, connecting the stub housing via an extension to the accelerating chamber. L_D-L_H-L_{St} outer conductor of coaxial resonator system. *k* oscillator connection. *O* oscillator housing. *Q* compartment containing the cooling-water hoses. Sp_1 and Sp_2 coils of cyclotron magnet.

is supported only at the flange *F* by which it is connected to the accelerating chamber. This prevents floor vibrations, due to the operation of pumps, etc., from being transmitted to the stub housing and the tuning fork, and the housing is able to follow changes in the position of the main mass of the cyclotron (see above) without strains being set up. Deformations of the housing itself do not affect the accurate

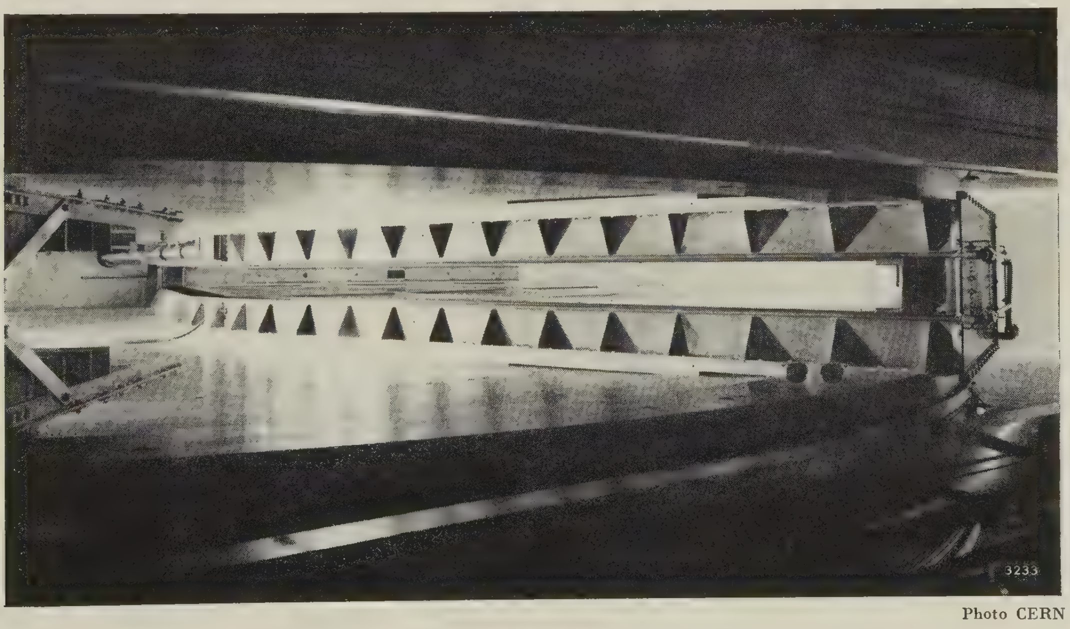

Photo CERN

Fig. 15. View of the dee, mounted between the pole plates. Note the relatively narrow mouth of the dee. To reduce the high demands on the stability of the orbits of the particles in the vertical direction, it would be a help to make the dee mouth wider. This has not been done, however, largely because of the small dee capacitance needed, which requires a large distance between the dee plates and the earthed outer conductor of the dee system. On the left, at the rear, the tube to which the ion source is attached can be seen projecting into the accelerating chamber.

maintenance of the mutual positioning of the tuning fork T (on the stub) and the associated stator S (on the stem), their position being constantly corrected by the feelers X and the suspension mechanism driven by servo motors A (see III, p. 176). To facilitate assembly and disassembly, a trolley is fixed underneath the stub housing, which can be lowered on to rails; after lowering this trolley and disconnecting the flange, the stub housing can be wheeled away.

Finally, a few comments on the assembly of copper plates which constitutes the outer conductor of the resonator (the liner). The part that surrounds the dee, L_{D}, and the dummy dee, D_2, are electrically joined to the pole-piece plates P_1 and P_2 and directly secured to them. The part L_{H} around the dee stem is at about the same distance from it as at the transition from the dee to the stem. The side walls of these sections of the outer conductor are formed by perforated copper plates. The outer conductor L_{St} of the stub is carried by steel girders, which are bolted to the inside of the stub housing.

The stub at the shorted end cannot be connected directly but only capacitatively to its outer conductor, the reason being that direct voltages of about 1000 V must be applied to the dee and dee stem and also to the stub in order to avoid a discharge. The capacitance of the shorting capacitor (C_{b} in fig. 14) should be high and its inductance low. This apparently simple circuit element caused quite a lot of trouble in the construction (see also the end of this article). Use was made for this purpose of commercial ceramic disk capacitors of 1000 pF. The capacitor was built up from 20 groups of 126 disks each (*fig. 16*). The total capacitance is 2.52 μF. The heat generated by the losses in the capacitor is removed by cooling water. During operation the maximum permissible direct voltage is 1500 V.

Fig. 14 also shows the tap connection k on the stub for the radio-frequency supply. By removing a few screws on the outside of the stub housing, this connection can be moved slightly in the longitudinal direction of the resonator for making initial adjustments. The RF generator with its transmitting valve is contained in a housing O, which is bolted to the bottom of the stub housing. For replacing the valve, it can be let down and wheeled away.

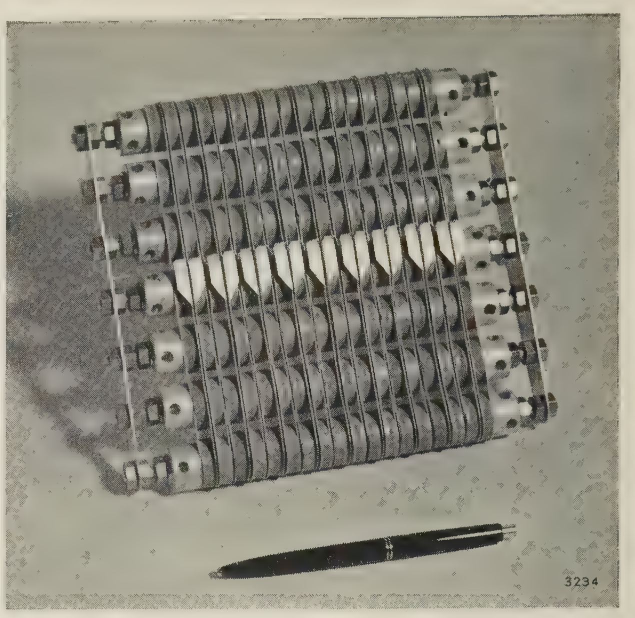

Photo CERN

Fig. 16. One of the twenty groups of ceramic capacitors from which the shorting capacitor C_{b} is built up.

The RF generator

The RF voltage for exciting the resonator is supplied by a triode oscillator, fitted with a water-cooled triode TBW 12/100 [6]). Even taking all possible losses into account (see p. 151), the power reserve of this 100 kW valve is very appreciable. As we shall see, this triode is particularly suitable for use in a grounded-grid arrangement.

In view of the wide range in which the resonator frequency is varied, the circuitry and design of the oscillator is somewhat unconventional. The oscillator is required to operate stably in this whole range (and preferably only in this range, in order to avoid the possible excitation of parasitic oscillations). Tests on the full-scale model had shown that this was not possible in our case with the conventional feedback circuit generally used in synchrocyclotrons; see *fig. 17*.

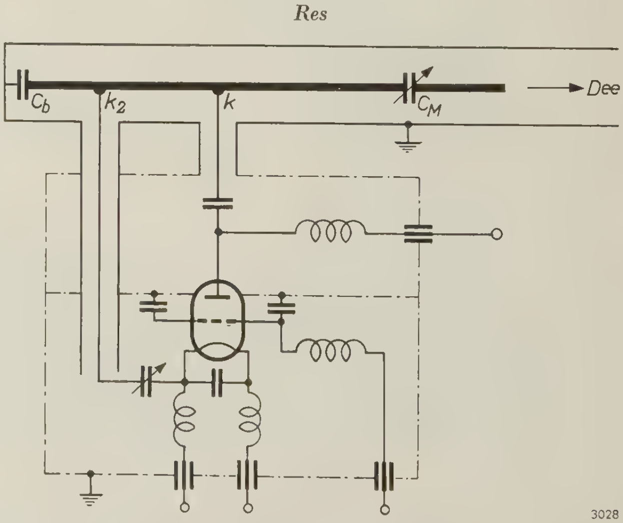

Fig. 17. Oscillator with conventional feedback circuit, as ordinarily used in synchrocyclotrons. The anode is connected at k to the resonator *Res*. Since the feedback voltage in this case is taken from a second tap k_2 on the resonator, a loop is produced which can easily give rise to unwanted modes of oscillation. (In its further details the circuit corresponds to that in fig. 18.)

---

[6]) This valve was described in Philips tech. Rev. **14**, 226, 1952/53.

The primary reason is that the oscillator is liable to produce oscillations in the loop formed by the relatively long transmission lines to the two connection terminals on the resonator. Furthermore, this circuit makes it difficult to keep the feedback voltage in a suitable phase over the whole frequency range: the phase difference between anode and cathode voltage, which should be zero in the ideal case, becomes so large at the extreme frequencies that the oscillation condition for this circuit can no longer be satisfied.

A circuit that proved highly satisfactory is the one represented in *fig. 18*. The oscillator here is excited by a feedback voltage taken from an inductance L in the anode circuit, but it is the resonator, which is connected at only one point, that determines the frequency. This virtue is attributable to the low losses (high wattless power) of the resonator (the Q is particularly high, > 2000). The resonator functions, as it were, like a flywheel: hence the term *flywheel circuit*. The fact that the resonator need be connected to only one point is also an advantage from the point of view of construction, since it calls for only one high-vacuum lead-in for RF current. Moreover, the feedback factor can now be adjusted by shifting the connection tap a in the oscillator itself, i.e. outside the vacuum tank, and the variation of the feedback factor with frequency can be controlled by the addition of circuit elements in the easily accessible feedback system. Since the grounded-grid arrangement, when properly designed, ensures the efficient internal decoupling of anode and cathode, the feedback is governed solely by the circuit elements outside the valve.

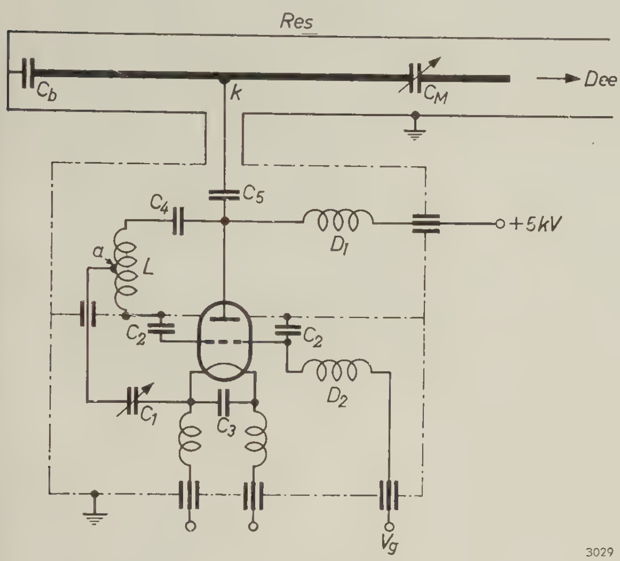

Fig. 18. Oscillator with flywheel circuit. The feedback voltage is tapped from a point a on the inductance L; the resonator *Res*, which is connected at only one point k, itself determines the frequency owing to its high Q, i.e. its high wattless power. The inductances of the tube and supply lines are compensated by means of the remotely controlled variable capacitor C_1 in order to ensure that the alternating voltage on anode and cathode are exactly in phase. The capacitor is adjusted such that this is achieved at the centre frequency of the resonator frequency swing. C_2 capacitor for RF earthing of the grid, C_3 for shunting the filament. C_4 and C_5 anode-voltage blocking capacitors. D_1 and D_2 chokes.

This arrangement proved to be so effective, particularly in the avoidance of parasitic oscillations, that it was subsequently adopted by Philips for the 150 MeV cyclotron in Paris.

If the anode circuit, which in fig. 18 consists of an inductance L shunted across the resonator, is to act as a resonant circuit, the resonator proper must possess capacitative reactance in the relevant frequency range. The frequency of the oscillator is therefore always slightly above the natural frequency of the free resonator. Because of the high quality of the resonator, however, the difference is negligibly small.

The self-inductances of the valve and its connections tend to give rise to differences between the alternating voltages applied to anode and cathode, which theoretically should be in phase. These inductances are compensated by a capacitor C_1, which consists of two variable vacuum capacitors connected in parallel. Of course, the compensation can only be perfect at one particular frequency. When the cyclotron is in operation, this frequency is held in the middle of the modulation range. For this purpose, one of the vacuum capacitors can be varied from the control room, 60 metres away from the cyclotron (see I). The phase deviation at both ends of the modulation range is relatively small, owing to the relatively low Q of the cathode portion of the feedback circuit (which, as we have seen, does not determine the frequency).

We shall now briefly consider some other details of the design. The TBW 12/100 triode is built in such a way as to allow an effective separation between the cathode and anode of the oscillator, as required in a grounded-grid arrangement. To this end the oscillator housing is divided into two parts by a horizontal partition at the level of the grid connection. Extremely effective RF earthing of the grid is achieved by fitting the partition with 96 ceramic capacitors of 1000 pF each, arranged in a circle around the valve (C_2 in fig. 18). Care was taken to avoid resonances from these capacitors in the range between 16 and 29 Mc/s. The same type of capacitor is used for shunting the filament (C_3). The coils used for the inductance L in the anode circuit and the choke D_1 in the anode-voltage supply line are of tubing through which an air current is passed for cooling. A ceramic pot capacitor C_5 is included in the anode connection on the resonator for DC blocking. The line for the connection is kept as short as practical, and special arrangements are made to keep the inductance of the capacitor connections very small, so that the RF oscillator voltage is transmitted to the resonator with as little attenuation as possible.

Apart from the usual electrical screening with sheet copper, the generator housing is surrounded by a sheet-steel housing to shield the valve from the stray field of the cyclotron magnet (which would adversely affect the mutual conductance). For the same reason the anode can is enclosed in a 10 millimetre thick iron tube. For insulation from earth the cooling water is again passed through a double hose of polyvinyl chloride about 10 m long.

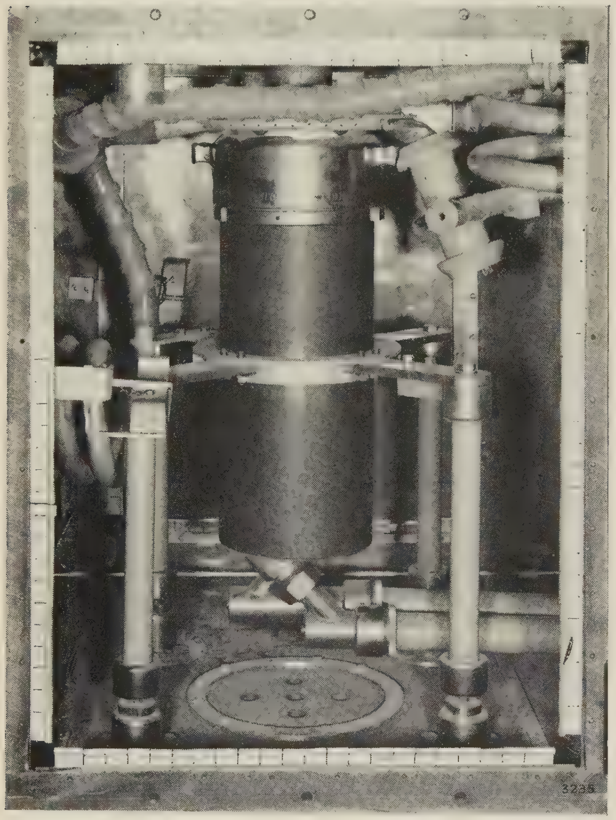

Photo CERN

Fig. 19. View inside the generator housing. Centre, the anode can with cooling jacket; top right, the feedback coil, consisting of three turns; left, one of the chokes.

Fig. 19 gives a view of the interior of the generator housing, showing some of the components mentioned. The normal operating data of the oscillator are presented in *Table I.*

Table I. Oscillator data for normal pulsed operation.

Anode voltage	5-6 kV
Anode current (average value)	3-4 A
Grid current (average value)	1-1.5 A
Duty cycle (fraction of modulation period)	60-70%
Frequency sweep	16.5-29 Mc/s
Anode efficiency	59-62%

Ancillary equipment

The radio-frequency system also comprises power supplies, a cooling installation for the cooling water, a device for pulsing the cyclotron, and instruments for controlling and monitoring the system. All this ancillary equipment, which is more or less conventional in design, is housed separately from the cyclotron in the power house which contains the converter set supplying the current for the large magnet (*fig. 20*; see *El* in fig. 3 in I). The RF system can largely be operated and controlled from here instead of from the master control room (fig. 5 in I). The operating controls are interlocked in such a way as to safeguard the system from damage due to manipulating the controls in the wrong order. The main switching operations can be checked on panels both in the master control room and in the converter room *El*. These operations include switching on and off the filamant current for the HT rectifier and for the oscillator valve; switching on and off the anode voltage; raising and lowering this voltage, and also the direct voltage for dee and stub; switching on and off the tuning-fork modulator and raising or lowering its amplitude. The equipment is provided with elaborate safety devices: all major faults are individually signalled, and if dangerous faults arise the relevant part of the installation is automatically switched off.

The object of the above-mentioned pulsed operation of the cyclotron is to obviate needless thermal loading, in particular of the modulator: the oscillator need only operate during that portion of the modulation period in which particles can be accelerated. The oscillator is controlled by pulses applied to its grid. The requisite switching pulses are supplied by the tuning fork itself (III, fig. 25). The fairly elaborate equipment required for producing the pulses and for effecting synchronization with the tuning fork or with external pulses (e.g. for experiments with a bubble chamber) will not be discussed here.

During the operation of the cyclotron the RF system has caused no particular difficulties. At certain frequencies, dips sometimes appeared in the amplitude curve of the dee voltage, and to compensate for these the anode voltage had to be chosen somewhat higher than normal (6 kV). It was soon discovered that these dips were attributable to reso-

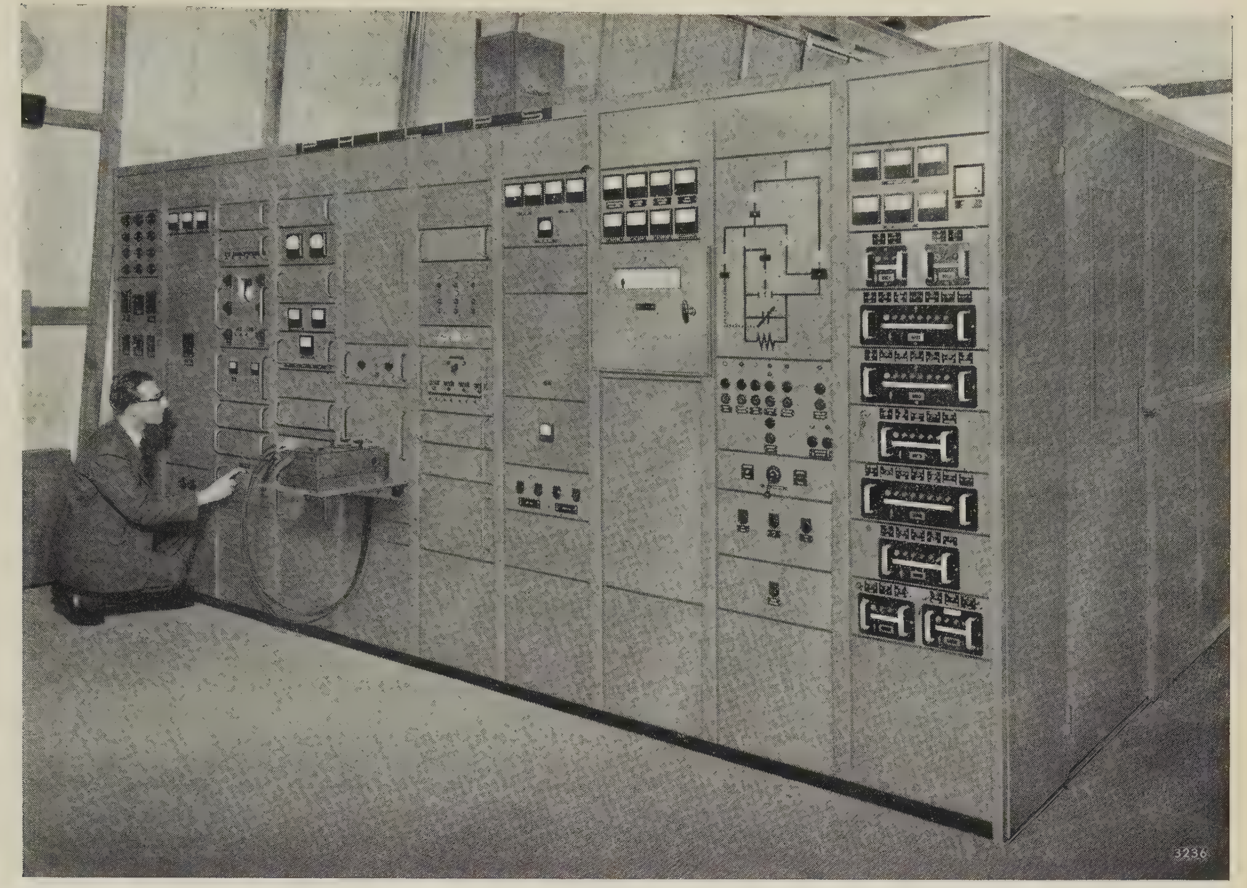

Photo CERN

Fig. 20. Part of the control and monitoring equipment for the RF system.

nance frequencies from the stub shorting capacitor (C_b in fig. 14). Since the properties of the ceramic dielectric of this capacitor were somewhat temperature-dependent, the occurrence and location of the dips in the curve depended markedly on the time during which the cyclotron had been in operation and on the cooling of the capacitor. Not much could therefore be done about these dips. While the synchrocyclotron was shut down for a while, however, the original shorting capacitor was replaced by another ceramic capacitor specially designed for this purpose, and consisting of only a few large plates.

Summary. The RF system of the CERN synchrocyclotron, developed and built by Philips Eindhoven, in cooperation with CERN engineers, contains two main components which are briefly described. These are the resonator and the RF generator, with elaborate ancillary equipment. The required proton energy of 600 MeV calls for a very large frequency sweep, from 29 to 16.5 Mc/s. The tuning-fork capacitor used for this frequency modulation provides a capacitance variation between 256 and 2580 pF. By combining this capacitor with an inductance ("stub") to form a series resonant circuit, a dee system could be designed whose resonant frequency varies between the above-mentioned limits. Some underlying theoretical considerations are discussed, and details given of the design work on the dee system, for which three different models were used. The voltage and current distributions on the resonator at the highest and lowest frequencies are given on the assumption of an RF supply voltage of constant amplitude. The voltage amplitude at the dee mouth is shown to be considerably greater during the whole modulation period than accords with the "ideal" amplitude programme (for a phase $\varphi = -30°$ of the accelerated particles). The construction of the resonator system is then described, mention being made of the measures taken to avoid mechanical strains in the resonator resulting from deformations in the cyclotron. The circuit chosen for the oscillator is a "flywheel" circuit, not previously used in cyclotrons (using a water-cooled 100 kW triode TBW 12/100 oscillating valve). The essential feature of this circuit is that the control voltage for the valve is taken from a feedback circuit in the oscillator, although the resonator — which is connected at only one point — still determines the frequency, owing to its high Q. This circuit largely overcomes the troubles experienced from parasitic modes of oscillation in the RF system, which have been such a source of difficulties in other cyclotrons. The construction of the oscillator is briefly discussed, and passing mention is made of the ancillary apparatus, including the equipment for pulsing the cyclotron.

III. THE TUNING-FORK MODULATOR

by B. BOLLÉE *) and F. KRIENEN **).

621.376.32:621.384.611.2

The function of the modulator in the RF system of the CERN cyclotron is to cause the frequency of this system to swing periodically (55 times per second) from about 29 to 16.5 Mc/s (wavelength 10.3 to 18.2 metres). The frequency modulation in a synchrocyclotron is commonly effected by means of a rotating capacitor. The RF voltage which thereby appears on the bearings and on the vacuum-tight lead-in to the rotating shaft can, however, give rise to considerable difficulties. Another method is based on the use of a varying inductance, consisting of a coil with ferrite core whose permeability is varied by passing a periodically varying premagnetizing current through an auxiliary winding. In the present case it was to be foreseen that this method would flounder on the magnetic losses in the ferrite. These considerations led to the trial in the CERN machine of a new method of frequency variation hitherto little used in synchrocyclotrons, namely the use of a vibrating capacitor [1]). The development of this system was entrusted to the Philips Laboratories at Eindhoven, in 1952, that is before the official foundation of the CERN.

First we shall give here a broad description of the system that was finally evolved after lengthy experiments. Numerous difficulties had to be overcome before arriving at the present satisfactory results. We shall then go on to discuss in more detail the structural design, the drive mechanism and the cooling of the vibrating system, together with various subsidiary problems.

Outline of the vibrating capacitor system

The varying capacitance of the modulator is achieved by means of a vibrator in the form of a tuning fork, the prongs of which encompass a stator (see *fig. 1*).

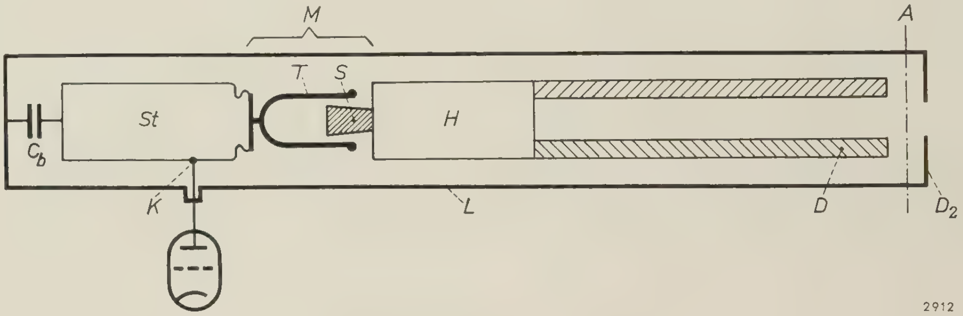

Fig. 1. The radio-frequency system of the CERN synchrocyclotron may be regarded as a coaxial transmission line. *A* centre line of the cyclotron (position of ion source). *D* dee. D_2 dummy dee (earthed). *H* stem of dee. *M* modulator, with tuning fork *T* and stator *S*. *St* "stub" (end section of transmission line). *L* outer conductor of transmission line. *K* coupling to anode of oscillating valve. C_b capacitor giving RF connection of stub to outer conductor but enabling the stub to be brought to a DC potential with respect to earth (see II, p. 158).

Between the prongs of the tuning fork and the stator a voltage of 10 to 20 kV is applied. In view of the risk of flash-over, it was desirable to make the distance between the prongs and the stator not less than 1.5 mm. This meant that the prongs of the tuning fork had to be made very wide in order to achieve a sufficiently high maximum capacitance. This was also desirable for other reasons: the density of the RF current over the prongs had to be small enough to allow adequate removal of the heat thereby generated. The prongs of the tuning fork, or the *blades*, as we can now better call them, are therefore 2 metres wide, which was roughly the maximum width allowed by the available space between the two vacuum pumps of the accelerating chamber (see part I, fig. 7). The stator, situated symmetrically between these blades with an overlap of 10 cm, is a 2-metre long aluminium girder bolted to the stem of the dee. Limitations were also imposed on the other

---

*) Philips Research Laboratories, Eindhoven.

**) CERN, Geneva.

[1]) The 740 MeV synchrocyclotron at Berkeley in California, the world's largest, also uses a vibrating capacitor, though of different design (with vibrating tongues). See R. L. Thornton, CERN Sympos. 1956^{I}, p. 413; B. H. Smith, K. R. Mackenzie, J. Reidel *et al.*, Wescon Conv. Rec. I.R.E. **1**, 60, 1957.

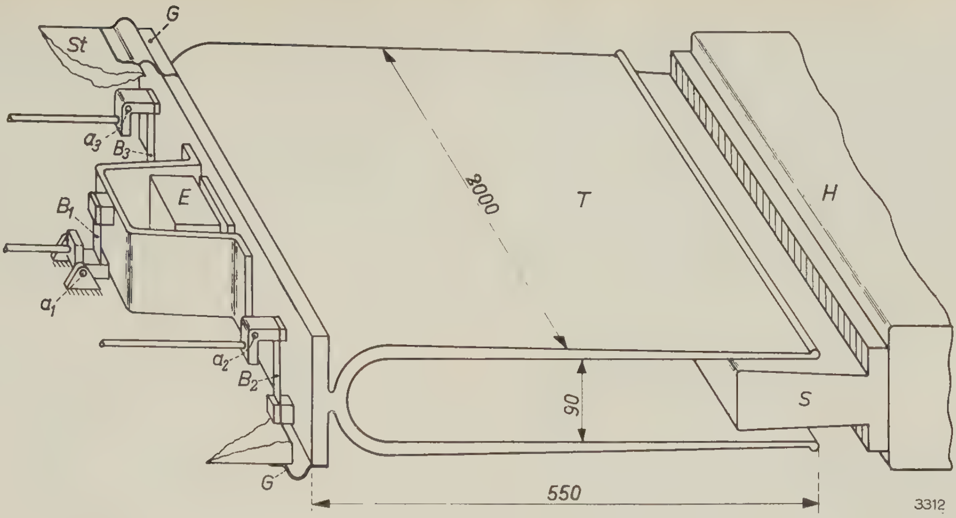

Fig. 2. Perspective sketch of tuning fork *T* and stator *S*. *H* dee stem. *E* drive mechanism. B_1, B_2, B_3 three steel strips on which the tuning fork is suspended. a_1, a_2, a_3 spindles on bearings in the stub frame. *G* leaf springs of beryllium bronze, fitted over the whole width of the tuning fork to effect electrical connection with the stub *St*.

dimensions of the tuning fork. The height was limited by the height of the vacuum chamber to about 20 cm; the length was limited to about 60 cm, having regard to the specified total length of the RF system and the optimum position for the coupling to the anode of the oscillating valve (see Part II, p. 154).

The tuning fork, which is attached by a short stem to a foot, was made from a solid block of aluminium to within an accuracy of $^1/_{10}$ mm. It weighs about 75 kg, and its natural frequency is 55 c/s. Further details of the shape and dimensions of the tuning fork are given in *fig. 2*, and *fig. 3* shows a photograph of the finished construction.

Fig. 2 illustrates how the tuning fork is set in vibration by an electromechanical converter, fixed to the foot. The operation depends on the converse of the well-known phenomenon that a vibrating tuning fork held to a sounding board transfers energy to the latter (and thereby becomes more audible). If, instead of the tuning fork, the sounding board is vibrated at the appropriate frequency, energy is transferred in the opposite direction and the prongs of the tuning fork are set in vibration. In the present case the foot — which acts as the sounding board — must be given a horizontal amplitude of about 0.15 mm if the blades are to vibrate at the required amplitude of 12.5 mm at each of the "lips". The tuning fork is mounted on steel suspension strips (B_1, B_2, B_3 in fig. 2), so that the horizontal movement is virtually unimpeded. The electrical connection to the stub (the end section of the resonator system, *St* in fig. 1) is effected by bent leaf springs (*G*) of beryllium bronze. No vibration energy of consequence is transmitted via the strips and leaf springs to the stub and its supporting insulators. The large amplitude of the tuning-fork blades is illustrated by the photograph in *fig. 4*.

We shall now consider the properties of the tuning fork as a capacitor. In the "closed" position the inner face of the blades is parallel to the surface of the stator, the spacing δ between them being 1.5 mm. The capacitance is then 2580 pF. In the "opened" position, measured at the lips, δ is 26.5 mm and the

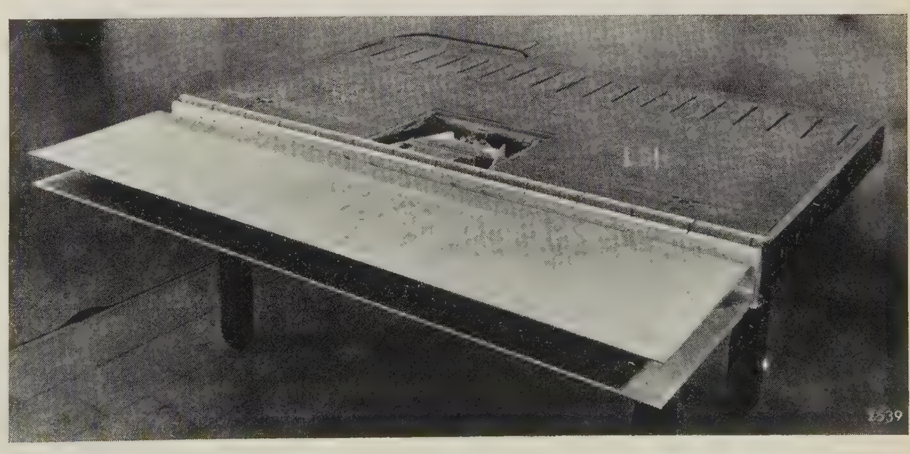

Fig. 3. The tuning fork mounted to the stub.

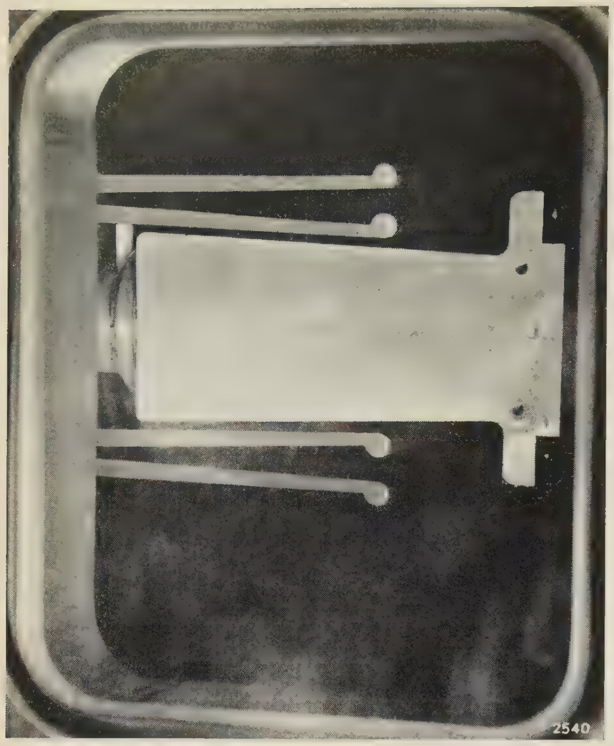

Fig. 4. Stroboscopic photograph, at 110 flashes per second, of the stator of the modulator and the overlapping ends of the blades of the vibrating tuning fork. Each blade is thus shown in its two extreme positions ("closed" and "open" state of tuning fork). Note the considerable amplitude of the blades.

capacitance 256 pF. These figures reveal that the relative variation of the capacitance (approx. 1 : 10) is considerably smaller than the relative variation of δ (approx. 1 : 18). This is due to the non-parallel motion and to the varying spread of the electrical field. This is evident from the pattern of the electrical lines of force and equipotential surfaces, from which the capacitance can be determined [2]); see *fig. 5a* and *b*.

If the synchrocyclotron is to function properly, the electrical oscillation frequency f of the RF system must fall successively from the maximum to the minimum value in accordance with a certain time function (see part II). The mechanical vibration of the tuning fork, i.e. the variation of the distance δ between the blades and the stator as a function of time, is sinusoidal. The variation of the capacitance C as a function of δ — between the two extreme values mentioned — is represented in *fig. 6a*. The variation of f as a function of C (fig. 6*b*) was found from calculations and from measurements on models of the RF system, where the vibrating capacitor was replaced by an adjustable plate capacitor. From

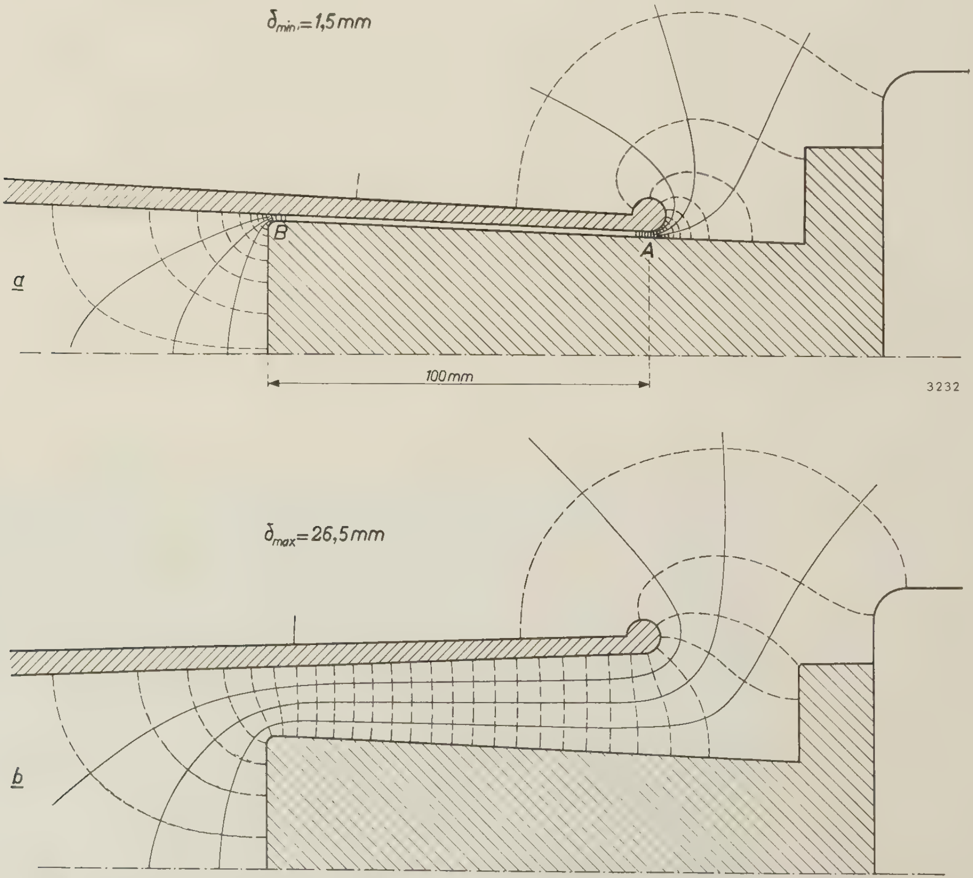

Fig. 5. Lines of force (dotted) and cross-sections of equipotential surfaces (solid lines) of the electrical field between the stator and one of the blades of the tuning fork, *a*) in the closed state, *b*) in the open state. In (*b*) the electrode faces are not parallel.

---

[2]) E. Weber, Electromagnetic fields, theory and applications, I. Mapping of fields, Wiley, New York 1950.

these three relations we can construct the resultant curve of f as a function of time. This is shown in fig. 6c.

Structures of such large dimensions as this cyclotron are always subject during operation to perceptible deformations due to variations of temperature and pressure, to magnetic forces, to elastic after-effects in vacuum seals, and so on. These deformations affect the relative position of stator and tuning fork. The amplitude of the tuning fork is also subject to a variety of changing influences, like the electrostatic forces between tuning fork and stator and the damping caused by eddy currents, which are induced in the moving blades by the stray field of the cyclotron magnet. Variations in these factors are unavoidable, since nuclear experiments with the machine require that it may be possible to vary not only the magnetic field but also the magnitude of the RF voltage and the length of time it is switched on. Since it is essential to the proper operation of the cyclotron that the relative position of stator and tuning fork, and also the amplitude of the latter, should not vary significantly during operation (e.g. less than 0.1 mm), in order to maintain the limits of the frequency variation, it was necessary to install elaborate control equipment. This equipment, which will be briefly described below, serves the additional purpose of protecting the tuning fork from damage: in the event of a fault, it switches off the drive and in some circumstances the RF oscillator also.

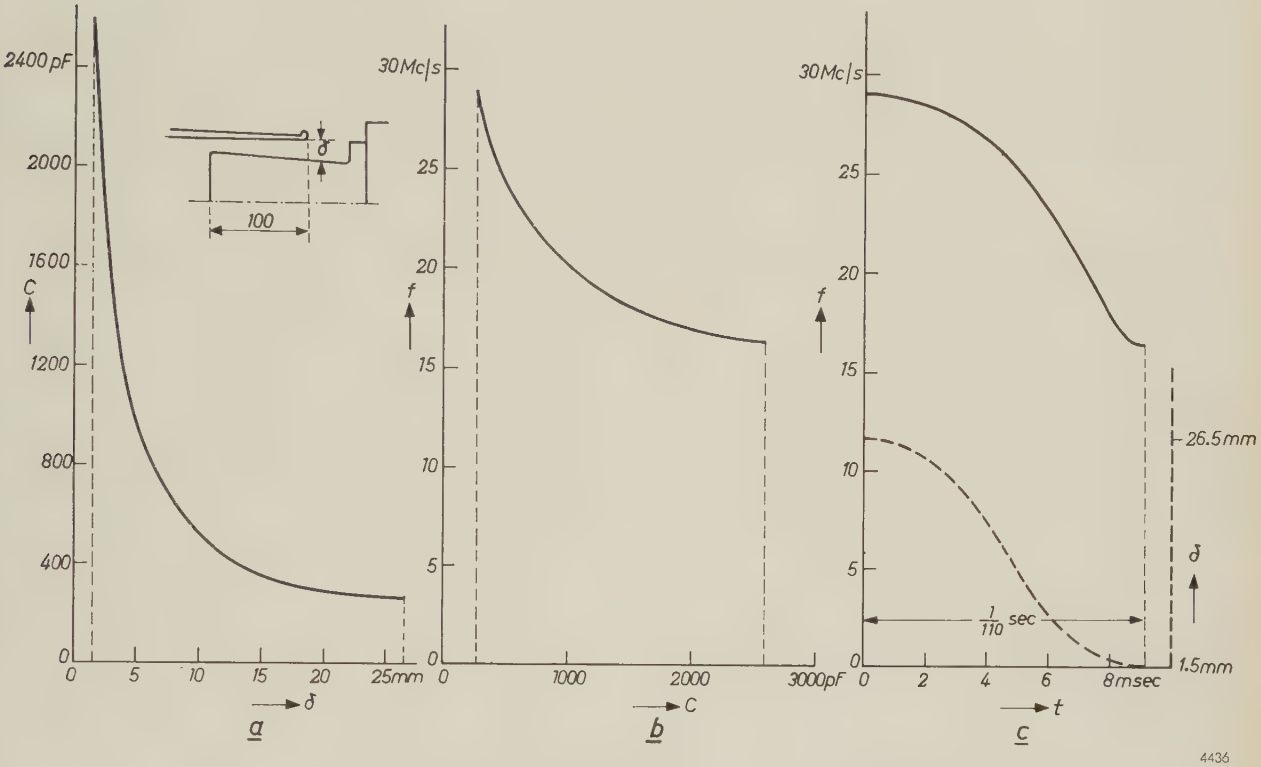

Fig. 6. *a*) Capacitance C of vibrating capacitor, as a function of the distance δ between the blades and the stator.
b) Oscillation frequency f of the RF system as a function of C.
c) Variation of oscillation frequency f with time t, during one modulation period. This relation is derived from (*a*) and (*b*), assuming δ varies sinusoidally with time (dashed curve).

When the cyclotron is operating, the RF current on the outer surface of each blade, and also on the inside near the stator, is of the order of 1000 amperes. The removal of the heat generated by this current created various problems, which we shall also consider at some length.

Mechanical design of the tuning fork

To illustrate the procedure adopted in designing the tuning fork, we shall take as our starting data a frequency of 55 c/s, the maximum and minimum capacitance required and the maximum available space of 200×60×20 cm. The tuning fork in its present form was developed in successive stages, partly empirically and partly on the basis of theoretical considerations stemming from the simple case of a vibrating bar of constant cross-section clamped at one end. It was necessary to take into account the material stresses and fatigue lifetime, the driving system, the weight and the method of support, the heating, and finally the problems of fabrication.

It will be useful first of all to confine our considerations to the form of the longitudinal section (the profile) of the tuning fork. The effect of the large width of the plates will be dealt with at a later stage.

The vibrating cantilever bar

When a uniform bar of free length l and thickness h, clamped rigidly at one end (*fig. 7*), vibrates in its fundamental mode with a maximum amplitude p, the maximum bending stress σ occurs at the place where the bar is clamped, and is given by:

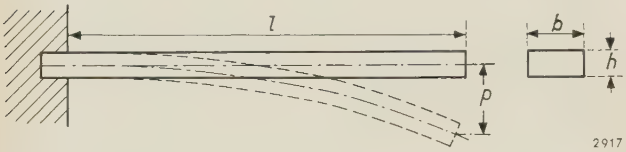

Fig. 7. Uniform bar clamped at one end. The width b of the cross-section is irrelevant to considerations concerning the amplitude p, the frequency f_m and the bending stress σ.

$$\sigma = 1.76 \frac{E\,h\,p}{l^2}, \quad \ldots\ldots \quad (1)$$

where E is the modulus of elasticity. The fundamental vibration (for which the bar deflects as in fig. 7) has the frequency

$$f_m = 0.162 \frac{c\,h}{l^2}, \quad \ldots\ldots \quad (2)$$

where c is the speed of sound in the bar material. From (1) and (2) we at once find the important relation:

$$\sigma = K_V \frac{E}{c} f_m p, \quad \ldots\ldots \quad (3)$$

in which the length and the cross-section of the bar have thus been eliminated. The numerical factor K_V is 10.9. We write the equation in this form because it is found to apply equally to vibrating bars of other longitudinal profile though with different values for the "form factor" K_V.

Before drawing conclusions from formula (3) we shall deal with the choice of material. From the points of view of fatigue strength and manufacturing possibilities, the choice lay between an aluminium alloy and a (non-magnetic) steel. The speed of sound c in both materials is roughly 5000 m/sec; thus according to equation (2) the same dimensions would apply to both cases. Aluminium was preferable because of its better electrical conduction, its lower mechanical damping and better workability, and the choice finally fell on an aluminium alloy, "Permandur", which possesses very high fatigue strength whilst retaining a reasonable electrical conductivity.

With reference to the bar, eq. (3) expresses the general fact that the natural frequency f_m and the amplitude p of a vibrating body cannot be raised independently, a limit being set by the permissible loading of the material. This is a problem encountered, for example, in mechanical sound-recording, where the problem is to record the highest audible frequencies with a reasonable amplitude [3]). It is perhaps surprising that, with our tuning fork, this problem arises at the relatively low frequency of 55 c/s. The reason is the very large amplitude required. The value of $p = 1.25$ cm was specified from an estimate of the capacitance variation obtainable with a vibrator as in fig. 7. If we substitute this value for p in eq. (3), taking f_m and c at the values mentioned and with $E_{Al} = 0.7 \times 10^6$ kg/cm², we find a bending stress of $\sigma = 1050$ kg/cm². This is much greater than the value of 600 kg/cm², which is regarded as admissible in the case of aluminium required to have a fatigue life of about 10^9 vibrations.

The fact that $p = 1.25$ cm at a frequency $f_m = 55$ c/s is a very large amplitude may perhaps best be appreciated by comparing the situation with that under static loading. For the bar to have the desired natural frequency it could be made, say, 1.5 cm thick and 46.8 cm long (see eq. 2). If the "bar" is given a width of 2 metres, like our tuning fork, the force that would have to act uniformly over its free edge to produce a deflection of 1.25 cm would be 4.4 tons.

With a uniform bar, then, it was not possible to meet the requirements.

As long ago as 1879 Kirchhoff showed that, given the same natural frequency and amplitude, the bending stress in bars of wedge-shaped profile (*fig. 8*) is substantially lower [4]). Eq. (3) is applicable here with the much smaller form factor $K_V = 2.78$. This would make it possible to achieve the desired capacitance variation with a bending stress of only 260 kg/cm². A "mathematical" wedge cannot be

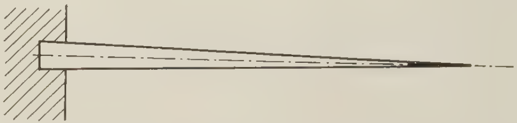

Fig. 8. Bar with wedge-shaped profile, clamped at one end.

---

[3]) See e.g. A. T. van Urk, The sound recorder of the Philips-Miller system, Philips tech. Rev. **1**, 135-141, 1936, formula (3).

[4]) G. Kirchhoff, Über die Transversalschwingungen eines Stabes von veränderlichem Querschnitt, Ann. Wiedemann **10**, 501-512, 1880.

used because a sharp edge would greatly increase the risk of electrical breakdown between vibrator and stator, quite apart from the manufacturing difficulties it would involve and its mechanical vulnerability. A compromise can be found, however, between the uniform and wedge shapes by giving the profile the form of a truncated wedge, the form factor for which will be between 10.9 and 2.78. The process of calculating the natural frequency and form factor of a bar of this shape is fairly complicated. The shape finally computed 5) is shown in *fig. 9*, the form factor for which is $K_V = 4.87$. The maximum bending stress is 460 kg/cm², which is well below the permissible value of 600 kg/cm².

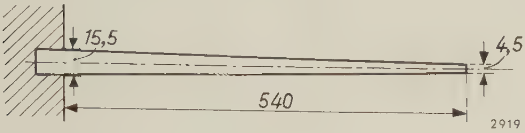

Fig. 9. Cantilever bar of truncated wedge profile chosen for the blades of the tuning fork.

For the interested reader we shall give a brief outline of the above-mentioned calculation. For a bar of density ϱ and of linearly-varying thickness as in fig. 9, whose cross-section at unit distance from the vertex of the mathematical wedge has an area A_0 and a moment of inertia I_0, the deflection y as a function of the distance u to this vertex is given by the differential equation 6):

$$4\pi^2 f_m{}^2 y = \frac{EI_0}{\varrho A_0}\frac{1}{u}\frac{\mathrm{d}^2}{\mathrm{d}u^2}\left(u^3\frac{\mathrm{d}^2y}{\mathrm{d}u^2}\right). \quad \dots\dots \quad (4)$$

Changing to the new variable

$$v = 2\pi f_m u \sqrt{\frac{\varrho A_0}{EI_0}}, \quad \dots\dots\dots \quad (5)$$

we can express (4) in the simpler form:

$$vy = \frac{\mathrm{d}^2}{\mathrm{d}v^2}\left(v^3\frac{\mathrm{d}^2y}{\mathrm{d}v^2}\right). \quad \dots\dots \quad (6)$$

It is easy to verify that all solutions of the differential equation

$$v\frac{\mathrm{d}^2y}{\mathrm{d}v^2} + 2\frac{\mathrm{d}y}{\mathrm{d}v} = y \quad \dots\dots \quad (7a)$$

satisfy (6) and the same holds for all solutions of:

$$v\frac{\mathrm{d}^2y}{\mathrm{d}v^2} + 2\frac{\mathrm{d}y}{\mathrm{d}v} = -y. \quad \dots\dots \quad (7b)$$

The general solution of (6) can therefore be written as a linear combination of the general solutions of (7a) and (7b), which are special forms of the Bessel differential equation. These solutions are:

$$y = \tfrac{1}{2}v^{-\frac{1}{2}}\left[A\mathrm{J}_1(2v^{\frac{1}{2}}) + B\mathrm{N}_1(2v^{\frac{1}{2}})\right]$$

and

$$y = -\tfrac{1}{2}v^{-\frac{1}{2}}\left[\mathrm{j}C\mathrm{J}_1(2\mathrm{j}v^{\frac{1}{2}}) + D\mathrm{H}_1{}^{(1)}(2\mathrm{j}v^{\frac{1}{2}})\right],$$

where J_1, N_1 and $\mathrm{H}_1{}^{(1)}$ are respectively first-order Bessel, Neumann and Hankel functions. With the new variable $w = 2v^{\frac{1}{2}}$ the deflection is finally given by

$$wy = A\mathrm{J}_1(w) + B\mathrm{N}_1(w) - \mathrm{j}C\mathrm{J}_1(\mathrm{j}w) - D\mathrm{H}_1{}^{(1)}(\mathrm{j}w). \quad .. \quad (8)$$

The four integration constants A, B, C, D have to be found from the boundary conditions. These are:

1) The angle of inclination $\mathrm{d}y/\mathrm{d}u$ at the clamped end = 0.
2) The deflection y at the clamped end = 0.
3) The bending moment, i.e. $\mathrm{d}^2y/\mathrm{d}u^2$, at the free end = 0.
4) The transverse force, i.e. $\mathrm{d}^3y/\mathrm{d}u^3$, at the free end = 0.

Substitution of these boundary conditions in (8) yields four homogeneous equations in the four constants. This system of equations has a solution only if its determinant, consisting of 16 Bessel functions, is zero. From the equation thus obtained one can determine, though rather laboriously, the eigen values w and hence, via eq. (5), the natural frequencies f_m. Of these we are only interested in the lowest frequency (the fundamental).

The bent bar

Even with the profile thus derived, the cantilever (wedge) bar — or rather, in view of its width, the cantilever (wedge) plate — is still not immediately a practical proposition. Noticeable deformation is unavoidable at the edges of the clamping blocks, with all the disadvantages this entails. Furthermore, powerful longitudinal forces as well as transversal forces act on the clamped end during vibration, and whilst the transversal forces might be balanced in our case, namely by using two plates vibrating in antiphase and clamped in the same block, longitudinal balancing is not readily possible. The latter forces are thus transmitted via the clamped end to the stub and to the accelerating chamber in the cyclotron.

It can be seen that these difficulties are circumvented by building the vibrator in the form of a tuning fork. This may be regarded as consisting of two bars, each having a profile as calculated above (fig. 9) but bent to form a half U. At the point where the two halves are "joined" (in reality, of course, the whole U-bar is made from a solid block of material) the same boundary conditions are realized as in the case of clamping. The difference, however, is that no forces whatsoever need be transmitted to the surroundings, since the tuning fork can be mounted on weak suspension springs. For the fundamental mode the tuning fork then vibrates as sketched in *fig. 10*.

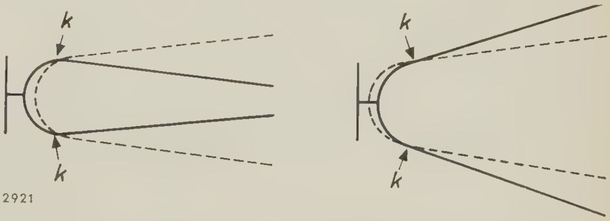

Fig. 10. Extreme positions of tuning-fork blades in the fundamental mode of vibration. The unexcited state is denoted by the dashed lines. Each blade has a "nodal line" at k.

---

5) See F. Krienen, Modulator CERN synchrocyclotron, CERN report 58-8, 23rd April 1958.

6) See e.g. J. W. Strutt (Lord Rayleigh), The theory of sound, Macmillan, London 1926 (2nd ed.), Part I, Chapter 8; P. M. Morse, Vibration and sound, McGraw-Hill, New York 1948.

The mode of vibration and frequency of the bar bent into a half U cannot be calculated exactly. Experiments show that the frequency of the bar is not much altered by the bending [7]). Investigation of the mode of vibration of a model (plate width 30 cm), using stroboscopic illumination, showed that there was not much change either in the deflections with respect to the centre plane of the bar profile. The important question remained, however, whether the bar would not be subject to considerably larger mechanical stresses σ at a given frequency f_m and amplitude p than the straight bar. Since the modes of vibration were the same, we drew the inference that the maximum kinetic energy was the same in both cases, and hence also the maximum potential energy (work expended on bending). But to infer from this that the stresses in the bent bar were the same as in the straight bar, we needed to be certain that the neutral plane (plane of zero deformation) remained in the centre plane of the bar profile during the vibrations of the bent bar, as it does in the straight bar. This was by no means certain; on the contrary, there was reason to believe that the neutral plane shifts, since it is known that this is the case for the deformation of thick rings, and since the major part of the bending energy of the U-bar is accumulated in the bent portion where it most resembles such a ring.

The simplest way out of this difficulty was to measure the stresses directly with the aid of strain gauges affixed to the inside and outside of the model. The largest alternating bending stress was found to be 370 kg/cm^2 on the outside, and 510 kg/cm^2 on the inside. These values were thought to allow a sufficient margin of safety, having regard to the "permissible" stress of 600 kg/cm^2. To make doubly sure, a 1 : 4 scale model was made in which, at a quarter the amplitude and a four times higher frequency (220 c/s), the same bending stresses arise. This model was subjected to a life test of 10^9 vibrations. The higher frequency reduces the length of the test to 52 days and nights, which the model withstood very satisfactorily.

In fact, it was these results that led to the decision to fix the modulation frequency at 55 c/s. It had been the aim to have as high a modulation frequency as possible, since this favours a high average proton current. Actually, the upper limit set to the repetition frequency by the requirement that the particles must have sufficient time to reach their final energy is considerably higher than 55 c/s (viz. above 100 c/s), as explained in Part II.

The actual dimensions of the tuning fork (fig. 2), which it was not yet necessary to include in these considerations concerning frequency, amplitude, mode of vibration and stresses, were established by the absolute magnitude of the capacitance to be achieved.

After these preparatory investigations, two tuning forks (one as a stand-by) were made with the required dimensions from two rolled blocks of aluminium. These blocks were ultrasonically tested for the presence of flaws. After machining, the tuning forks were finished by hand to an accuracy of 0.1 mm. In view of the marked effect which the state of the surface has on the fatigue strength, the bent part was polished on the inside and outside.

For the construction of the stator it was important to ascertain whether, in the closed state, the amplitude of the lips was sufficiently constant over the whole width of 2 metres. This again was checked stroboscopically. The amplitude, measured within 0.1 mm, was found to be constant within the permissible margin of 0.2 mm. The stator could thus be made in the form of a straight uniformly profiled bar. The profile had to be adapted to the shape of the tuning-fork blades in their closed position. The part of the blades involved (*A*-*B* in fig. 5) was found to remain straight within 0.1 mm.

Drive mechanism

From fig. 10 it may be inferred that the tuning fork will vibrate as required if the foot is caused to vibrate periodically in the direction of the axis of symmetry at a frequency equal to the fundamental frequency of the tuning fork. First thoughts perhaps suggest transferring the necessary alternating force to the foot by means of a rigidly mounted system, driven magnetostrictively, electromagnetically or electrodynamically (like a loudspeaker). Model tests soon made it clear, however, that the vibrations transmitted to the surroundings are prohibitive in the case of a rigidly mounted drive system. We may illustrate this by making an estimate of the necessary alternating forces — which, of course, are exerted as reaction forces on the support of such a rigid drive system. In the two blades of the tuning fork a vibration energy of about 60 joules is accumulated. From very rough model tests it was estimated that about $\frac{1}{2}$% of this energy is dissipated per vibration. The power to be supplied by the drive at a frequency $f_m = 55$ c/s was accordingly estimated at $P = 15$ W (see also below). Assuming that the driving power F is in phase with the velocity $\dot{x}$ at which the foot is displaced, we can write:

---

[7]) This has also been demonstrated theoretically for the prismatic bar (fig. 7); see C. H. Keulegan, On the vibration of U-bars, Bur. Stand. J. Res. 6, 553-592, 1931.

$$P = \tfrac{1}{2} \times 2\pi f_{\mathrm{m}} \hat{x}\ \hat{F}.$$

At the assumed amplitude of the lips (1.25 cm), $\hat{x} \approx 0.15$ mm, which yields $\hat{F} \approx 600$ newtons. In practice it is not generally possible to satisfy the above phase condition in full, so that the amplitude of the alternating drive force would be something like 1200 newtons (~ 120 kg).

Numerous other requirements and limitations made the drive system a difficult problem. The available space for the mechanism was restricted, the mechanism had to be readily replaceable in the event of a fault occurring, the heat generated (copper and iron losses) could effectively only be removed by conduction, because of the location in vacuo, for the same reason the use of sliding surfaces demanding lubrication was ruled out, and finally the drive had to operate at a position where the stray field of the cyclotron magnet was still fairly considerable.

The solution finally arrived at was an "internal" drive, utilizing an auxiliary mass which avoids a rigid mounting. The system is illustrated in *fig. 11*, and in the photographs of *fig. 12a* and *b*. An electromagnet with a laminated core is screwed to the foot of the tuning fork. The armature of the magnet, which acts as the auxiliary mass (further weighted by brass blocks to bring the total weight to 17 kg), is fixed to the foot by two very stiff springs of chrome-nickel steel; the resonant frequency of this system (auxiliary mass and springs) is virtually identical with the fundamental frequency of the tuning fork, 55 c/s. When the electromagnet is now energized with an alternating current of 27.5 c/s (half the resonant frequency, because the magnetic force is not reversed when the current changes direction), the tuning fork and the auxiliary mass are set in vibration in opposite phase at a frequency of 55 c/s. The amplitude of the relative displacement is about 1 mm. Because the system vibrates at its resonant frequency, the amplitude of the force F which the springs transmit to the foot of the tuning fork is about six times greater than the amplitude of the force F_{m} with which the magnet attracts the armature. The value $\hat{F} \approx 1200$ newtons can thus be reached with a reasonable energizing current.

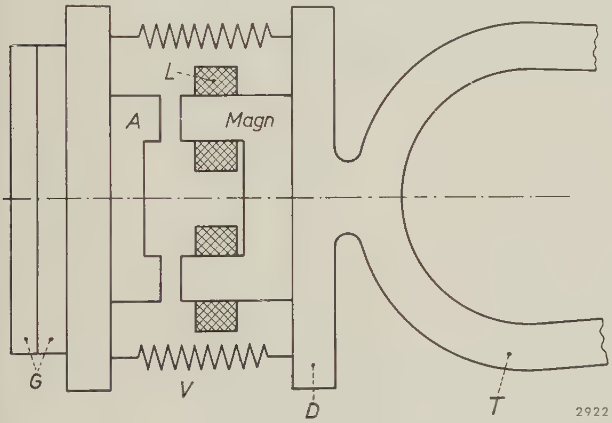

Fig. 11. Schematic representation of drive mechanism. *T* tuning fork with foot *D*, to which is mounted the electromagnet *Magn* with coils *L*. *A* armature, also connected to foot by springs *V*. The armature is weighted by brass blocks *G*. In reality, these are mounted partly around the magnet, owing to restricted space and also with a view to minimizing the bending moment acting on the springs.

For the coil windings, good use was made of a new Philips technique for winding enamelled wires, in which no paper insulation is needed and which gives a particularly high filling factor (85%) and good heat dissipation (1 W/m² per °C/m) *) — properties which were important here, where the magnet had to be accommodated in a limited space in high vacuum.

Mention should be made of the special form of the springs, shown clearly in fig. 12*a* and *b*. The fabrication of the springs from a single piece of material presented some difficulties, but the result justified the trouble taken. The springs have a highly constant stiffness of 1000 N/mm each, provide rigid clamping, and moreover their stiffness is relatively much greater in the transversal direction, properties insufficiently attainable with the more conventional helical spring and leaf-spring assemblies. A secondary advantage is their easy mountability. The bending stresses occurring are fairly high, up to 3000 kg/cm², which calls for a highly polished finish to avoid premature fatigue failure due to surface discontinuities.

We shall briefly describe the method of working out the required mass of the auxiliary mass, the spring stiffness and the magnetic force. For this purpose the system consisting of tuning fork and drive mechanism was replaced by the model represented in *fig. 13*. M'' is the auxiliary mass, S'' the stiffness of the chrome-nickel steel springs. The friction B'' represents the hysteresis and eddy-current losses of the electromagnet and the deformation losses of the springs. The continuously distributed mass of the tuning fork is replaced by two concentrated masses M and M', corresponding to the parts lying respectively between, and outside (on either side), the nodal lines of the fundamental mode of vibration (cf. fig. 10). Further, S' represents the lumped stiffness of the tuning fork, B the lumped mechanical damping of the mounting (fig. 2), which can be disregarded in the first instance, and B' allows for the internal damping of the tuning-fork material, for eddy-current losses in the stray field of the cyclotron magnet, and, in some experiments done during the development, for viscous damping by the atmosphere (air or hydrogen gas). The quantities M, M', S' and B' were calculated from the fundamental frequency f_m, the total potential energy W of the vibrating tuning fork, and the measured power P absorbed at resonance. (It is found that M may be put equal to the actual mass of the whole tuning fork, together with all parts rigidly mounted to it.) We now have the following three differential equations for the motion of the three masses:

---

*) *Editorial note:* We hope to be able in the near future to publish an article on this winding technique, which has already proved to be of value in many applications.

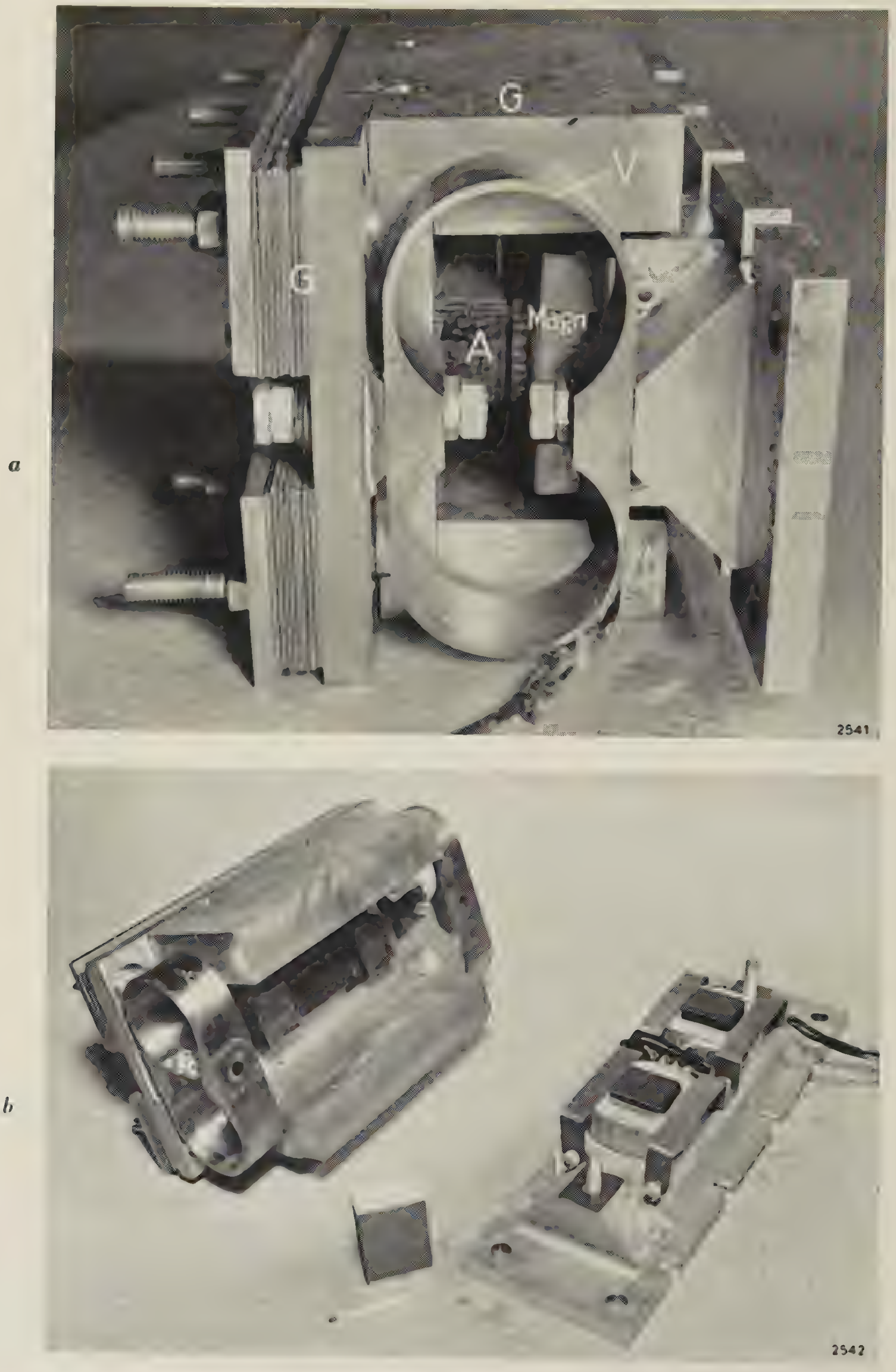

Fig. 12. *a*) Drive mechanism ready to be bolted to the foot of the tuning fork. Meaning of letters as in fig. 11.
b) The mechanism dismantled. Right, the electromagnet with coils on base plate; left, the auxiliary mass with laminated armature and springs.
The rectangular recesses in the edges of the base plate are for the cooling pipes, which remove the power dissipated in the electromagnet (about 30 W, see page 179).

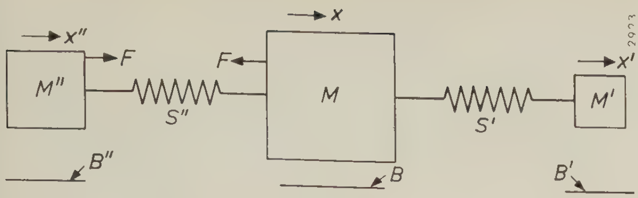

Fig. 13. Equivalent circuit of tuning fork and drive mechanism, for deriving the equations of motion and for studying the behaviour of the whole system.

$$\left.\begin{aligned} M\ddot{x} + B\dot{x} + S'(x-x') + S''(x-x'') &= F_{\mathrm{m}}, \\ M'\ddot{x}' + B'\dot{x}' + S'(x'-x) &= 0\,, \\ M''\ddot{x}'' + B''\dot{x}'' + S''(x''-x) &= -F_{\mathrm{m}}\,. \end{aligned}\right\} \quad . \; . \; (9)$$

With the aid of these equations, the behaviour of the vibrating system was examined in detail. In particular, the force F acting on the foot of the tuning fork, and given by:

$$F = F_{\mathrm{m}} + S''(x''-x), \quad . \; . \; . \; . \; . \quad (10)$$

was calculated for varying conditions. We shall mention here only one rather unexpected result of these calculations, namely that stable operation is best ensured if the natural frequency of the system formed by the two masses M and M'' and the spring S'', is about 0.5 c/s lower than the resonant frequency of the whole system. This was also confirmed experimentally.

To avoid the excitation of unwanted modes of vibration, and the needless dissipation of energy in the coils (which would complicate the removal of heat in the vacuum), the magnetic force on the armature should possess no higher harmonics of the fundamental frequency, i.e. it should be purely sinusoidal. The form of the energizing current needed for this purpose is by no means sinusoidal, since the magnetic force at a given current is still highly dependent on the length of the air gap of the magnet, which varies during the vibration. This is illustrated in *fig. 14.*

The energizing current with the required waveform is obtained by supplying the sinusoidal voltage from an *RC* oscillator to a push-pull amplifier in class C operation. The natural frequency of the *RC* oscillator is roughly 27.5 c/s. As the tuning fork vibrates, one of the blades reflects the light from a stationary electric bulb, thereby transmitting periodic flashes to a photocell. The voltage pulses thereby produced are used to synchronize the *RC* oscillator. As a result of this feedback, which is automatically kept in the correct phase, the tuning fork vibrates precisely at its fundamental frequency.

The photocell signal is also used for synchronizing the periods during which the RF oscillator for the cyclotron is switched on: so that no energy shall be wasted, the RF oscillator is operated only in that half of each modulation period during which the particles can be usefully accelerated (*f* decreasing). Moreover, the signal can be used to synchronize the ion source — if the latter is pulsed — and any other devices that may be involved in experiments with the particle beams.

Parasitic modes of vibration

The mode of vibration in which we are interested — the fundamental mode of the tuning fork — is purely two-dimensional. For this reason, in the foregoing, we have mainly had to concern ourselves with the *profile* of the tuning fork. However, its third dimension (its width of 2 metres) may give rise to three-dimensional modes of vibration, such as occur in membranes and plates. By exciting the tuning fork at its various resonant frequencies, and

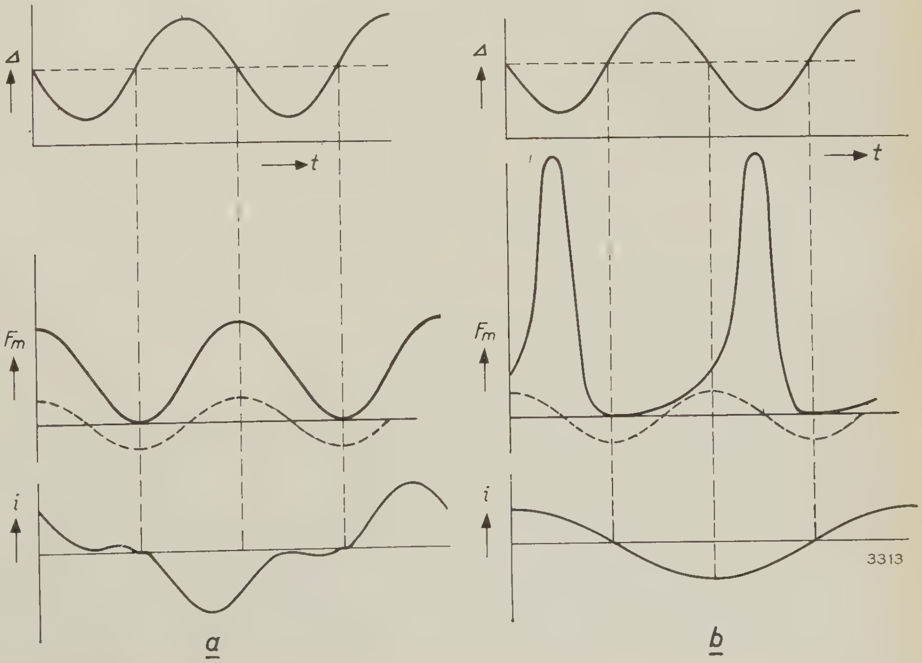

Fig. 14. Electrical supply for drive mechanism. From top to bottom are shown, as a function of time t: the relative displacement of the armature (length Δ of air gap), for which a sinusoidal variation is assumed; the magnetic attractive force F_{m}; the current i for energizing the electromagnet. The dashed curve represents the velocity of the armature.

Curves (*a*) relate to a current waveform designed to produce a sinusoidal variation of the magnetic force. Curves (*b*) represent the case of a sinusoidal current; the magnetic force here is badly affected by higher harmonics of the fundamental frequency.

sprinkling sand on to the plates, Chladni's figures can be produced of the different modes of vibration (see *fig. 15*) [8]. If the natural frequency of a particular mode of vibration is equal or almost equal to a multiple of the fundamental frequency, this vibration may be directly excited by the driving force or via an internal coupling with the fundamental mode of vibration (e.g. due to the Poisson contraction). It is then superposed on the fundamental vibration, thereby upsetting the operation of the modulator.

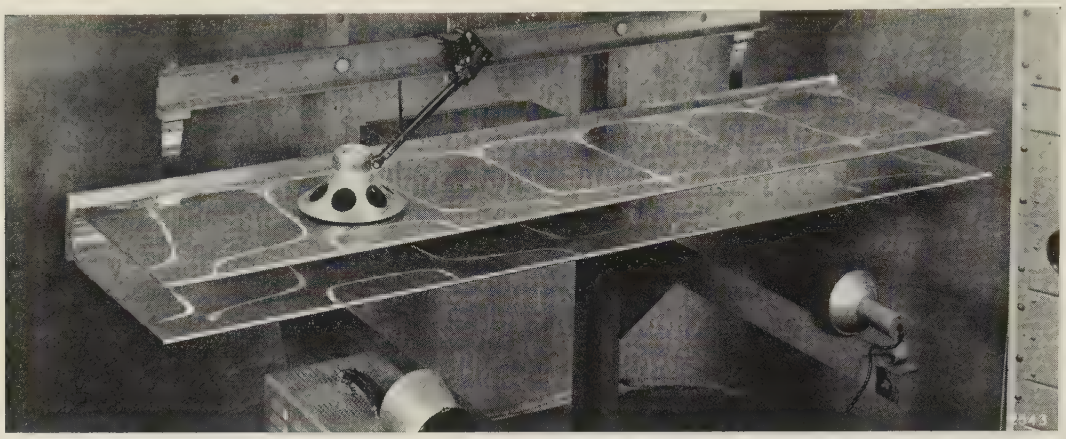

Fig. 15. Chladni's figure obtained when the tuning fork is made to vibrate in a particular undesired mode by excitation with the appropriate resonant frequency [8].

The chance of such a dangerous coincidence of frequencies is small, but we did in fact happen to stumble on it. To illustrate the counter-measures adopted, we shall examine the possible modes of vibration at somewhat greater length.

We denote the modes of vibration by two index figures, which indicate for a single blade of the tuning fork the number of nodal points at the sides (but not counting the inevitable fundamental node near the foot, see fig. 10) and at the front edges, respectively. We also add to these figures an *s* or an *a*, depending on whether the two blades vibrate symmetrically or anti-symmetrically (see *fig. 16*); both cases are possible, since anti-symmetric vibration does not shift the centre of gravity of the system as a whole. In this notation, *s00* is the fundamental mode of vibration, which is the one we want. *Fig. 17* illustrates various modes of vibration together with their resonant frequencies, measured on a 1 : 4 scale model of the tuning fork. (We are concerned only with vibration modes of the first kind, i.e. forms without node at the sides, since modes with side nodes are found to have much higher frequencies which are not troublesome.) It can be seen in fig. 17 that the frequencies of the modes *a04* and *s04* are fairly close to twice the frequency of *s00*. With the actual tuning fork, mounted in the vacuum tank, the frequency of the *s04* mode was even more troublesome than in the model; it was this mode that gave rise to the trouble referred to above. This occurred particularly when the tuning fork was warming up (see next section). The effect of heating causes a slight shift of all resonant frequencies — not so much because of the expansion of the material but because of the drop in the modulus of elasticity. At a particular tem-

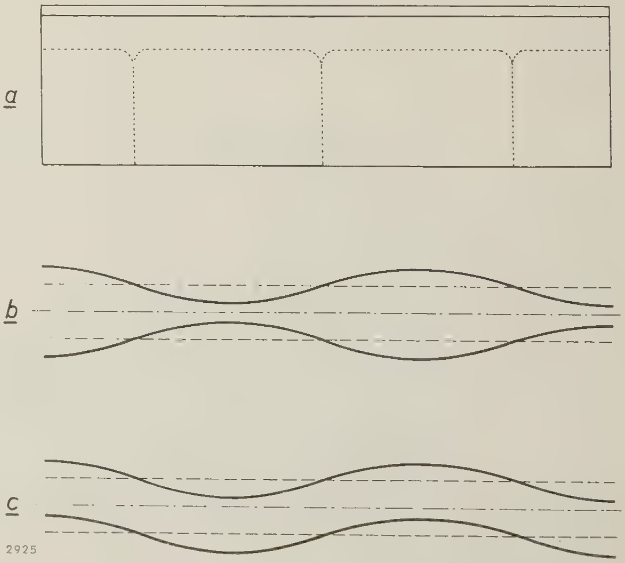

Fig. 16. *a*) Chladni's figure of a vibration of the tuning fork, with three nodes at the front edge and none at the sides of the blades (except the fundamental node as in fig. 10). The two blades can vibrate here in two modes: symmetrically (*b*), called the *s03* mode; or anti-symmetrically (*c*), mode *a03*.

---

[8] A short account of these was published some time ago in this journal: B. Bollée, Chladni's figures on the vibrating capacitor of a synchrocyclotron, Philips tech. Rev. **19**, 84-85, 1957/58.

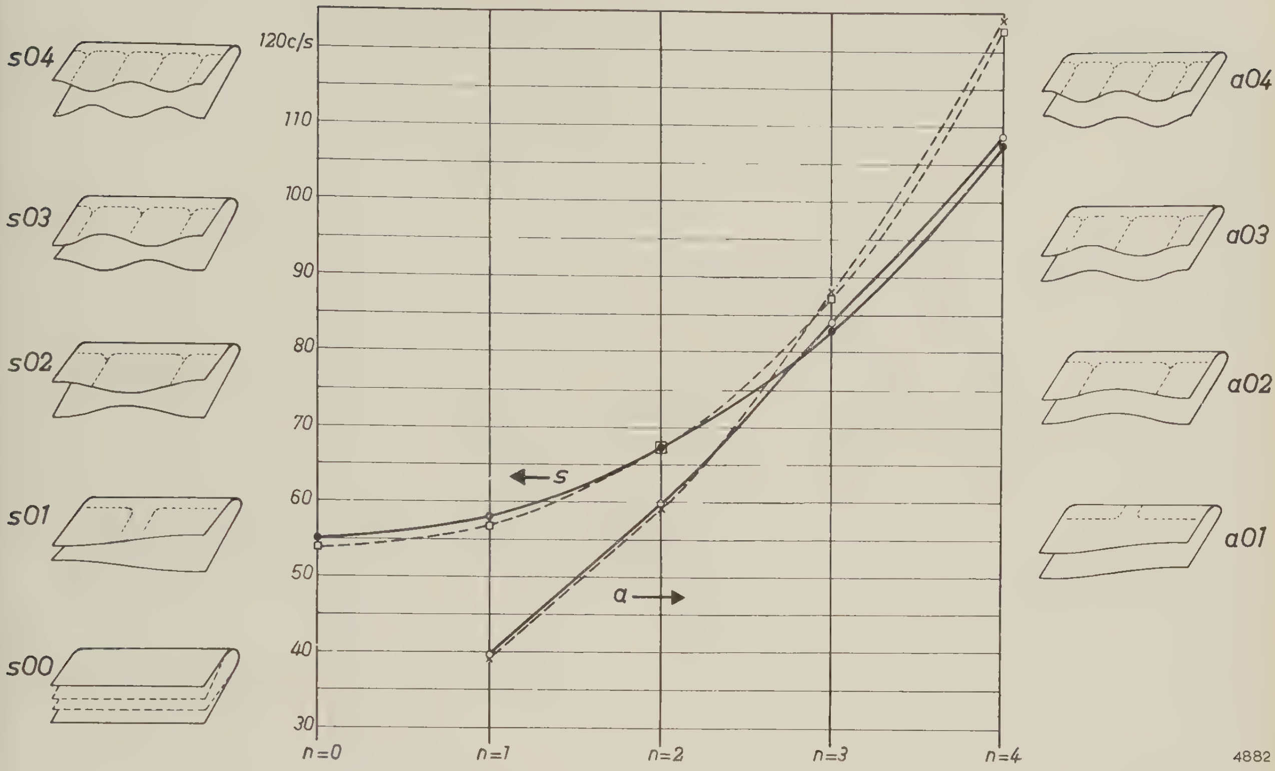

Fig. 17. Resonant frequencies of the modes of vibration "of the first kind" (i.e. without nodes at the sides of the blades, first digit = 0), for $n = 0$ to 4. The black dots pertain to symmetrical modes of vibration, the open circles to anti-symmetrical modes. These modes, *s00* to *s04* and *a01* to *a04*, are illustrated at the sides of the graph. The solid curves drawn through the points have no physical significance in the sections between the whole values of n; they were useful, however, in enabling us, after finding the first three resonant frequencies, to find the others: the resonances are so sharp (width of resonance curves of the order of 0.01 c/s) that they are easily missed.

The dashed curves show the resonant frequencies of the tuning fork when stiffening ribs are fitted, as in fig. 18. The small squares pertain to symmetrical modes, the crosses to anti-symmetrical modes of vibration.

perature distribution, the *s04* vibration came to resonance.

Apart from making a new tuning fork with modified dimensions, which was obviously not an attractive proposition, there were various possible ways of dealing with this interference, namely: artificial damping, "decoupling" by cutting slots into the blades, and finally shifting the dangerous resonant frequency by reducing the width of the blades or by mounting a stiffening rib on each of them.

After careful consideration of the drawbacks and risks of these measures and the time they would probably cost, the choice fell on the stiffening ribs. *Fig. 18* shows how the rib is mounted over the whole width of a blade. It was necessary to secure the ribs with particular care, since they undergo accelerations of 120 g during vibration. Of course, the ribs not only change the ratio of the fundamental frequency to the frequency of *s04*, but also to the frequency of all other modes of vibration. The chance that this will give rise to other resonances can, however, be minimized, for it can be shown that, at the temperature distributions found in practice, no troublesome resonances will occur provided that all resonant frequencies, assuming a ***homogeneous*** temperature distribution, differ by at least one per cent from any neighbouring whole

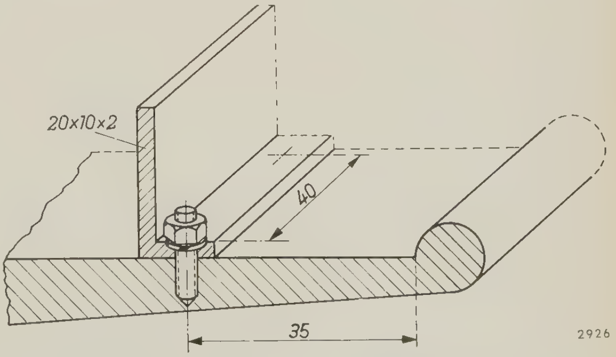

Fig. 18. Location and form of the stiffening rib mounted to each of the two blades to prevent the excitation of undesired modes of vibration. (The ribs are clearly visible in fig. 24.)

multiple of the fundamental frequency. This follows from an estimate concerning the expected effect of the locally varying decrease in the modulus of elasticity, and concerning the (very small) width of the resonance curves for the various modes of vibration. With the aid of data derived from a model, the approximate displacements of all resonant frequencies, brought about by the stiffening ribs, was calculated for various positions and dimensions of the ribs. In this way the dimensions and location were determined which satisfy the above 1% condition (fig. 18). After the ribs had been fitted, no further undesired resonances were encountered. As a consequence of the increased weight the fundamental frequency itself dropped to 54 c/s, and it was necessary to adjust the drive mechanism accordingly.

It would be going too far to describe here the method of calculation adopted. It should be mentioned, however, that the solution of the problem, although it apparently concerns a minor detail, had a decisive bearing on the success of the whole modulator project.

Cooling the tuning fork

Part of the tuning fork (AB in fig. 5) functions as a variable capacitance in the RF system and thus carries an RF current (instantaneous frequency f). For various reasons it was necessary to give very careful consideration to the removal of the heat thereby generated. We shall go into these reasons and discuss the solution adopted.

The heat likely to be generated can be fairly accurately calculated. Since the length of the tuning fork is small in relation to the wavelength, the current flowing in the tuning fork may be regarded to a good approximation as quasi-stationary. This current is given by:

$$\hat{I} = \frac{\hat{U}_{\mathrm{D}}}{\zeta} \sin \frac{2\pi f l}{c}, \quad . \quad . \quad . \quad . \quad (11)$$

where l is the distance between the tuning fork and the dee mouth, ζ is the characteristic impedance of dee and dee stem, U_{D} the voltage at the dee mouth and c the velocity of light. $\hat{U}_{\mathrm{D}}$ varies with the frequency f, from about 8 kV at 29 Mc/s to about 25 kV at 16.5 Mc/s. Given $l = 3.5$ m and the value $\zeta = 6$ ohms, as assumed at a preliminary stage of the design, it follows that $\hat{I}$ varies between 3100 and 1550 amperes. If s is the length and b the breadth of the tuning fork, d the penetration depth of the current and ϱ_{Al} the resistivity of the aluminium alloy, then the resistance is given by:

$$R = \frac{s\varrho_{\mathrm{Al}}}{2bd}. \quad . \quad . \quad . \quad . \quad . \quad . \quad (12)$$

We can fill in $s = 60$ cm, $b = 2$ m, $\varrho_{\mathrm{Al}} = 4.926 \times 10^{-8}$ Ωm at room temperature, but the penetration depth d also varies with the frequency, from 22 microns at 29 Mc/s to 29 microns at 16.5 Mc/s. The average power is found by integrating $\frac{1}{2}I^2R$ over one period of modulation, using the known time-variation of the frequency (fig. 6*c*) and taking into account that the RF oscillator is operated only for about half of every modulation period (see above). Graphic integration led to the value $P = 240$ W.

Apart from this electrical dissipation, some heat is also generated by the mechanical losses in the vibrating tuning fork, but these losses are roughly estimated, as mentioned earlier, at only about 15 W.

The removal of a dissipated power of some 250 W from the large surface of the tuning fork would be a simple matter if convection were possible; in a vacuum, however, it becomes a problem. Relying on the large surface area, one might in the first place think of removing the heat by radiation. A simple calculation shows that this is not a feasible solution. The total radiating surface may be put at $2 \times 200 \times 60$ cm^2 (the heat spreads easily enough throughout the tuning fork). Between the copper outer conductor of the RF system and the aluminium tuning fork the temperature difference should be such as to allow a heat transfer of about 0.01 W/cm^2. Having regard to the absorption coefficients of copper and aluminium (both of which are about 0.2), we arrive at a temperature rise of approximately 120 °C in the aluminium. Such a temperature rise is out of the question. Not only would it reduce the natural frequency of the tuning fork by about 1 c/s, thereby somewhat changing the tuning with the drive (see the frequency condition mentioned on page 171, at the end of the small print), but what is more, the material of the tuning fork would not be able to withstand it: at temperatures above about 100 °C, slow changes in the metallographic structure of the aluminium alloy can occur, as a result of which the material loses its favourable properties.

An attempt to improve the radiation cooling by artificially blackening the tuning fork and the copper outer conductor (thus increasing the absorption coefficient) came up against practical difficulties. Black anodizing of the tuning fork is ruled out because of its known disastrous effect on the endurance limit. To spray on a black coating is rather risky because the coating might flake in the long run or give off gases in vacuo, and also because it might make things even worse by increasing the generated heat (owing to dielectric losses).

It was therefore decided to remove the heat not by radiation but by water-cooling. This meant that cooling pipes had to be fitted to the foot of the tuning fork. Now, however, we were faced with another danger. The non-uniform cooling gives rise in the tuning fork to a temperature gradient which, by causing non-uniform expansion and consequent mechanical stresses, might easily warp the blades. This would have the most serious consequences on the capacitance variations and on the operation of the positioning control (see the next section). An inquiry was therefore made into the temperature distribution and deformation to be expected in each of the blades.

The temperature distribution can be calculated to a good approximation by treating the profile of the tuning fork as a *linear* truncated wedge, as in its mechanical design (see fig. 9), having a length equal to the path along which the heat-flow takes place to the cooling pipes. The calculated temperature curve is shown in *fig. 19*. A correction has been applied here to allow for the effective constriction at the stem of the tuning fork, and allowance is also made for the heat generation on the inside of the blades near the stator, which was not taken into account in the power calculation given above. *Fig. 20* shows the heat streamlines and the contours of equal temperature. (Following the rules of field theory [2]), a sketch like this can be drawn simply by inspection, and with some practice and patience the result is often just as accurate as by calculation, and takes very much less time than measurements on an electrolytic tank, for example.) The outcome shows that a temperature difference of less than 13 °C was to be expected between foot and lips. As regards the deformations caused by this temperature difference, it was necessary to experiment on a full-size tuning fork. For this experiment the tuning fork (not vibrating) was set up in an air atmosphere, the foot being kept at room temperature by the cooling pipes, whilst the whole surface was artificially heated by strips of electrically conductive paper which were stuck to the outer surface of the blades with an insulating underlayer of thin nylon fabric

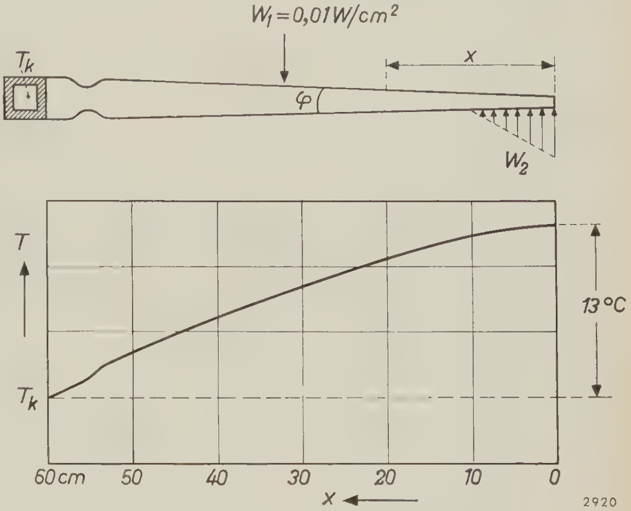

Fig. 19. Variation of temperature T over the profile of a tuning-fork blade, calculated by treating the profile as a straight truncated wedge with a constriction at the stem of the tuning fork. From the outer surface a power W_1 (= 0.01 W/cm²) goes inwards, and from the inner surface a power W_2 (at the position of the stator). The foot of the tuning fork is kept at the temperature T_k by a cooling-water pipe.

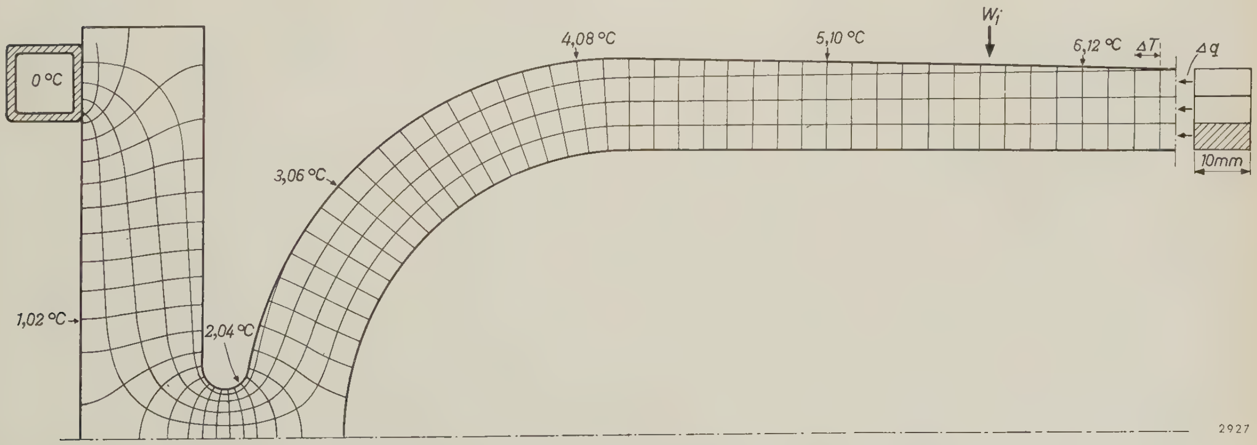

Fig. 20. Streamlines of heat-flow and equal-temperature contours in the profile of a blade of the tuning fork (only the curved section is reproduced, the temperature variation in the straight section being almost linear). In each stream tube (shown hatched in cross-section) a power Δq flows of 0.14 W. Since only the temperature differences are important here, the temperature in the cooling-water pipe (top left) is assumed to be 0 °C.

(*fig. 21*). By supplying each of the strips with a suitable current, the theoretically derived temperature gradient was fairly accurately simulated. It was found that the lips of the blades were less straight and parallel than when the temperature of the tuning fork was uniformly raised. The deviations were not readily reproducible, presumably because of various residual mechanical stresses in the rolled and machined plates, but they were so small (no more than about 0.2 mm) that they do not have any adverse consequences.

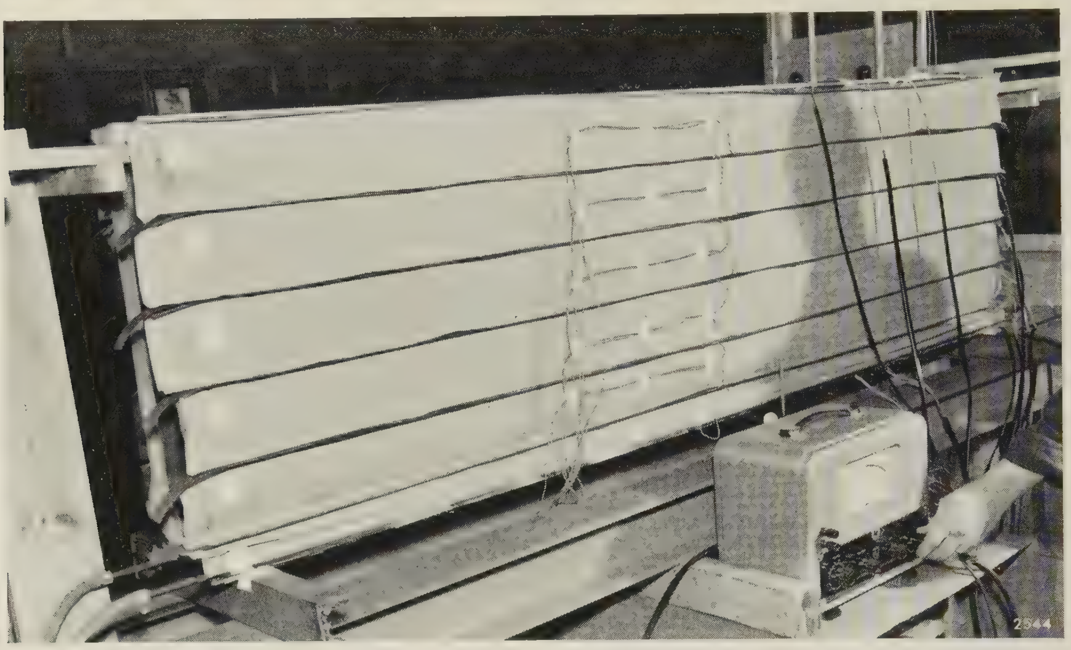

Fig. 21. Experimental arrangement for measuring the expected deformations of the tuning fork as a result of heating during actual operation, where only one end (the foot) is cooled with flowing water. The calculated temperature distribution is simulated by heating the blades with strips of electrically conducting paper, each fed with a specific current.

Fig. 22 shows the tuning fork mounted to the stub; note the flexible connections for the cooling pipes along the foot of the tuning fork.

It should be pointed out that in the foregoing we have considered the temperature distribution in the stationary state. The time constant of the process of heating and cooling the tuning fork is calculated to be about 1700 seconds. This means that each point of the tuning fork will have reached $\frac{2}{3}$ of its final value about half an hour after switching on the cyclotron.

Automatic positioning control

In the introduction we referred to the deformations that occur in the whole RF system when the cyclotron is in operation, and to the fact that the correct position of the tuning fork in relation to the stator must be maintained in spite of these deformations. There are two possible changes in their relative position: changes in the overlapping of tuning fork and stator, which amounts nominally to exactly 10 cm over the whole width; and changes in the "gap", by which we mean the distance within which the vibrating blades can approach the stator at any point. In the ideal case the position and the amplitude of vibration are so regulated that the gap at all points is 1.5 mm.

The relative horizontal displacements caused by deformations are of the order of 1 mm. They have hardly any effect on the gap but only on the overlapping, which causes no noticeable change in the capacitance *variation*. As regards the relative position of tuning fork and stator in the horizontal direction, it was therefore thought to be sufficient to make an adjustment once and for all when installing the modulator in the system at Geneva. To facilitate this adjustment, the three suspension points on the tuning fork are mounted to carriages, which can be slid over a distance of 5 mm (fig. 22).

The relative displacements that cause changes in the *gap* can be analysed into three movements (see *fig. 23*): *a*) vertical displacement of the tuning fork; *b*) turning of the tuning fork about an axis parallel to the lips; *c*) turning of the tuning fork about the centre line of the whole RF system. We may add to these *d*) incorrect vibration amplitude of the tuning fork. To correct the changes in the gap resulting from these deviations it was necessary to introduce, as mentioned in the introduction, an automatic positioning control system. This operates with three servomotors, which cause vertical displacement of the three suspension points (by pivoting about the spindles a_1, a_2 and a_3, respectively, in fig. 2). By suitably actuating the servomotors, separately or simultaneously, the three movements *a*-*c* can be effected and compensated. The three servomotors can be seen on the front face of the stub tank in the title photo of Part I. A fourth servomotor, whose shaft is coupled with a potentiometer which controls the energizing current for the tuning-fork drive, is used to keep the amplitude of the tuning fork at the correct value (*d*).

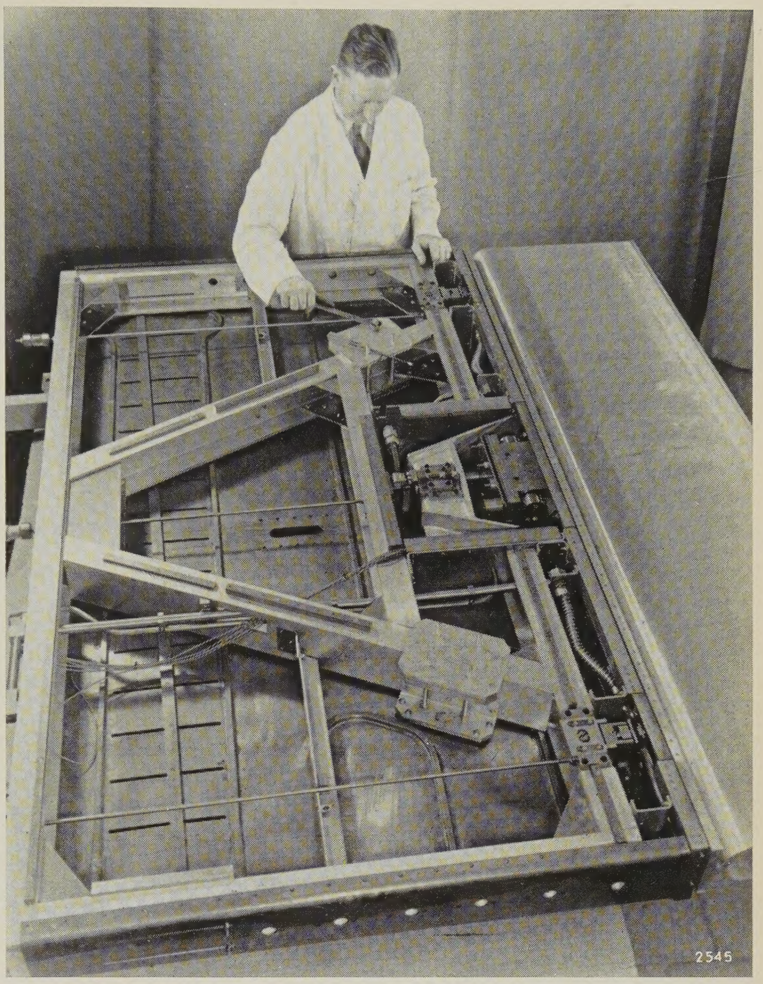

Fig. 22. The tuning fork (right) mounted to the stub, the top plate of the latter having been removed. Note the flexible connections for the cooling-water pipes, fitted to the foot of the tuning fork. The drive mechanism can also be seen, with the three rods which connect the points of suspension to the servomotors for the position control (see fig. 25 and fig. 2).

The four servomotors are controlled by a system which operates roughly as follows. The situation as regards the gap between tuning fork and stator is explored by feelers attached to the stator. There are altogether five such feelers, made of "Teflon" (*fig. 24*), each of which, if touched by the tuning fork, breaks an electrical contact. Three feelers are mounted directly on the end of the stator (two of these are visible in fig. 24, the third being about 2 metres away at the other end of the stator). From time to time, these three feelers, upon a "command" from the control system, can be slid further out of their metal sheaths in two steps of 0.1 mm by a small electromagnet. If one of these feelers is touched in its fully withdrawn position, the control system immediately switches off the oscillator, for in that case the gap is less than 1.4 mm, which was considered both mechanically and electrically dangerous. If the tuning fork touches one of the three feelers only after the first step, then the gap at that position is between 1.4 and 1.5 mm; if a feeler is touched only after the second step, the gap is between 1.5 and 1.6 mm; if a feeler is not touched at all, the gap is greater than 1.6 mm. The twenty-seven possible signal combinations from these three feelers correspond to various kinds of deviations from the desired situation, namely of type *a* or *c* (or *d*) or combinations thereof. By means of a "translator" in the control system, each of the signals sets in momentary operation that combination of servomotors which leads to the cor-

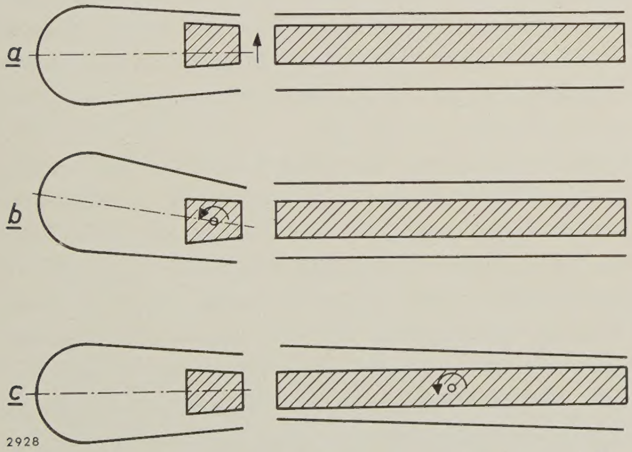

Fig. 23. The various misalignments in the position of the tuning fork relative to the stator. The arrows indicate the necessary corrections.
a) Vertical displacement.
b) Turning about an axis parallel to the lips.
c) Turning about the centre line of the RF system.

rection of the relevant deviation. The two Teflon feelers not yet discussed are mounted on an extension piece (partly visible in fig. 24) on the stator so that they check on the tuning fork at a point 100 mm nearer its foot than the first three. If one of these feelers is touched, the "translator" — depending on the information received from the first three feelers — actuates the servomotors in such a way that deviations of the type *b* or *d* are corrected.

Fig. 25 shows a highly simplified block diagram of the control system. A photograph of the control racks can be seen in *fig. 26*. The block diagram also indicates the frequency control, earlier mentioned, for the drive mechanism of the tuning fork, which is also responsible for synchronizing all the relevant parts of the cyclotron [9]).

Proving the modulator

It was not possible to say whether the modulator in all its complexity would come up to expectations until it had first been proved in the cyclotron itself, at Geneva, and then only after some months of normal operation. Various modifications were found to be necessary. In fact, some modifications had turned out to be desirable after the installation had passed through its preliminary trials at Eindhoven. In the latter tests the conditions of operation in the cyclotron could only be simulated to a limited extent, as far as the positioning in vacuo and the heating were concerned. The stub tank at Geneva was to be in communication with the accelerating chamber; at Eindhoven, after the tuning fork was mounted to the stub (fig. 22), the tank was provisionally sealed with a special cover plate to which the stator with built-in feelers was attached, and which was fitted with windows for observing the movements inside (*fig. 27*). The tuning fork was heated by twelve radiators each 2 metres long (the use of heating strips, as employed for investigating the deformation, was obviously not possible with the vibrating tuning fork because of the damping they would cause). The foot of the tuning fork was kept at room temperature by water-cooling. During the vibration of the tuning fork it was found necessary to make the back of the stub heavier with a block of lead weighing roughly 60 kg, the reason being that a resonance in the region of 50 c/s caused fairly considerable vibration of the stub together with its supporting insulators. The amplitude of the lips, measured with a stroboscope and cathetometer, showed local differences up to 0.3 mm. It was possible to reduce this deviation from straightness to about 0.15 mm by attaching a number of weights of 10 grammes to the ribs.

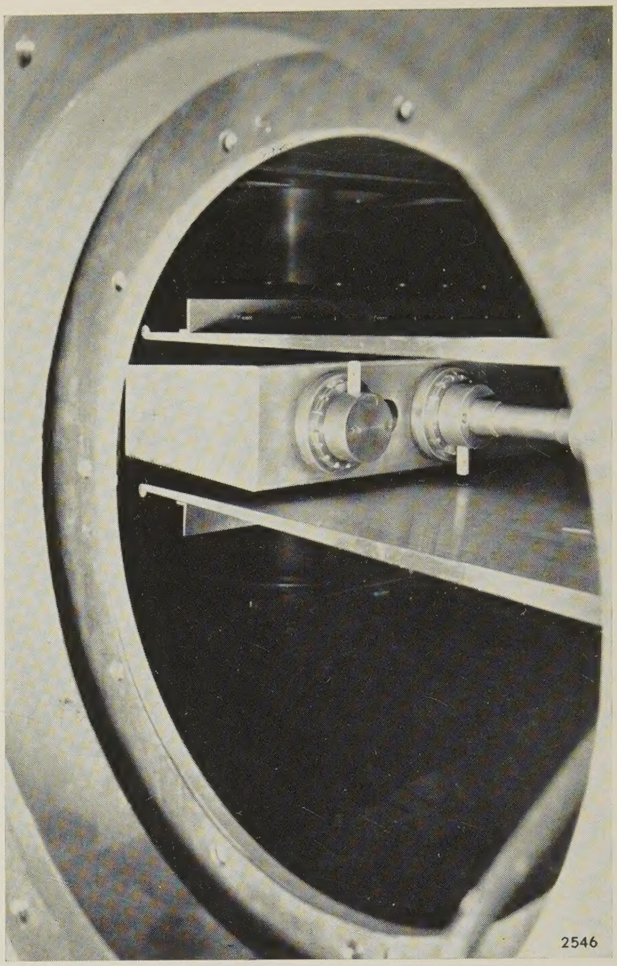

Photo CERN

Fig. 24. End of tuning fork and stator, mounted in the cyclotron and seen through a window in the accelerating chamber. The photograph shows two of the five "Teflon" feelers which are fitted to the stator for sensing the position and amplitude of the tuning fork.

In Geneva, however, other complications arose, in particular owing to the stray field of the large electromagnet of the cyclotron. The displacements of tuning fork and stator when the magnet was switched on were fortunately not too serious. Various components, like the feeler elements and filters in the control system which are within the stray field, had to be provided with better screening. The most disagreeable surprise, however, during the trial operation of the complete synchrocyclotron — in which only the ion source was not functioning, since of course no particle beams could be produced whilst people were still working inside the screened-

---

[9]) The tuning-fork modulator in its definitive form, as indeed the whole RF system for this cyclotron, was built under the direction of L. van Mechelen by a department of Philips Industrial Equipment Division at Eindhoven. Special mention is made of A. de Groot, now at the CERN in Geneva, who played an important part in the development of the control system for the tuning fork and of the entire electronic equipment for the RF system.

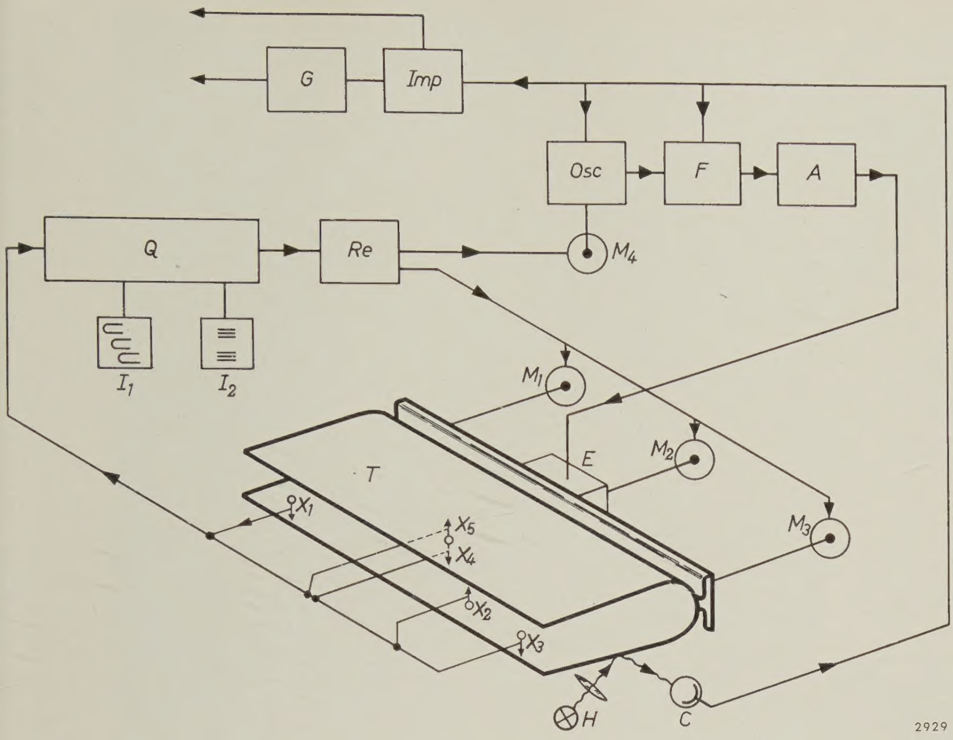

Fig. 25. Diagram of the system for automatically controlling the position and amplitude of the tuning fork. X_1-X_5 feelers fitted to the stator for sensing the situation of the tuning fork. Q "translator", which sets in operation the appropriate combination of the four servomotors M_1-M_4 via a series of relays *Re*, thereby operating the linkage for correcting the situation. I_1 and I_2 visual indicators. The three motors M_1-M_3 act on the suspension of the tuning fork T; M_4 acts on a potentiometer which controls the amplitude of the drive mechanism E. *Osc RC* oscillator, F phase-regulating circuit, and A amplifier for the drive system. H electric bulb and C photocell, which produce the feedback signal for frequency control in the drive system. This signal also serves for synchronizing the pulse generator *Imp*, which controls the RF generator for the cyclotron and (via G) the ion source and irradiation set-up.

off area — was occasioned by the energy losses in the tuning fork. Originally it was estimated that about 15 W would be needed to cover the losses due to damping, with perhaps the same wattage for the copper and iron losses of the electromagnet. During the trials at Eindhoven, with no electric or magnetic field, it was found that the damping consumed only 3 W, whilst the losses of the electromagnet were a mere 4 W. It therefore looked as if the drive mechanism, designed for about 30 W, was amply equipped for its task. In the proving run at Geneva, however, the drive mechanism consumed a total of 45 W! The reason turned out to be additional damping due to eddy currents produced in the blades of the tuning fork by a fairly strong horizontal component of the magnetic field at that position. A horizontal component of that strength had not been foreseen.

To reduce this component of the magnetic field an auxiliary winding was fitted around the stub tank, consisting of ten turns and carrying a current of 400 A. This reduced the eddy-current losses to about 6 W and the total power consumed by the electromagnet to about 30 W.

The RF voltage between stator and tuning fork, varying between 8 and 25 kV (see above), gave rise to no flashover. With a view to capturing stray ions, which can initiate discharges, stator and tuning fork were given DC potentials of —2200 and —800 V, respectively, with respect to earth.

The drift of minimum and maximum frequency as the tuning fork gets hot was found to be very slight indeed. The installation can also work for hours on end without the position control having to come into operation. The amplitude control comes

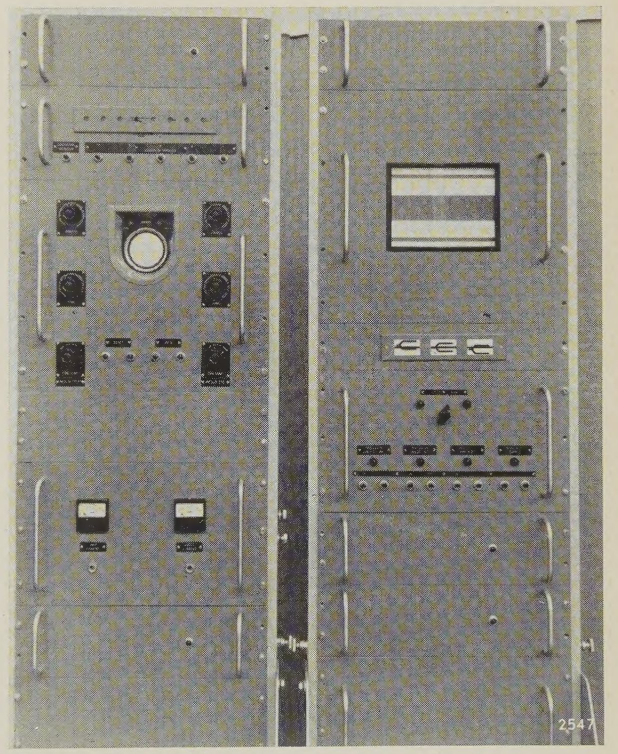

Fig. 26. Racks containing control equipment for the tuning fork. The panel on the right contains the instruments for visually indicating certain deviations in the position of the tuning fork: above, for deviation c; in centre, for deviation a; see fig. 23.

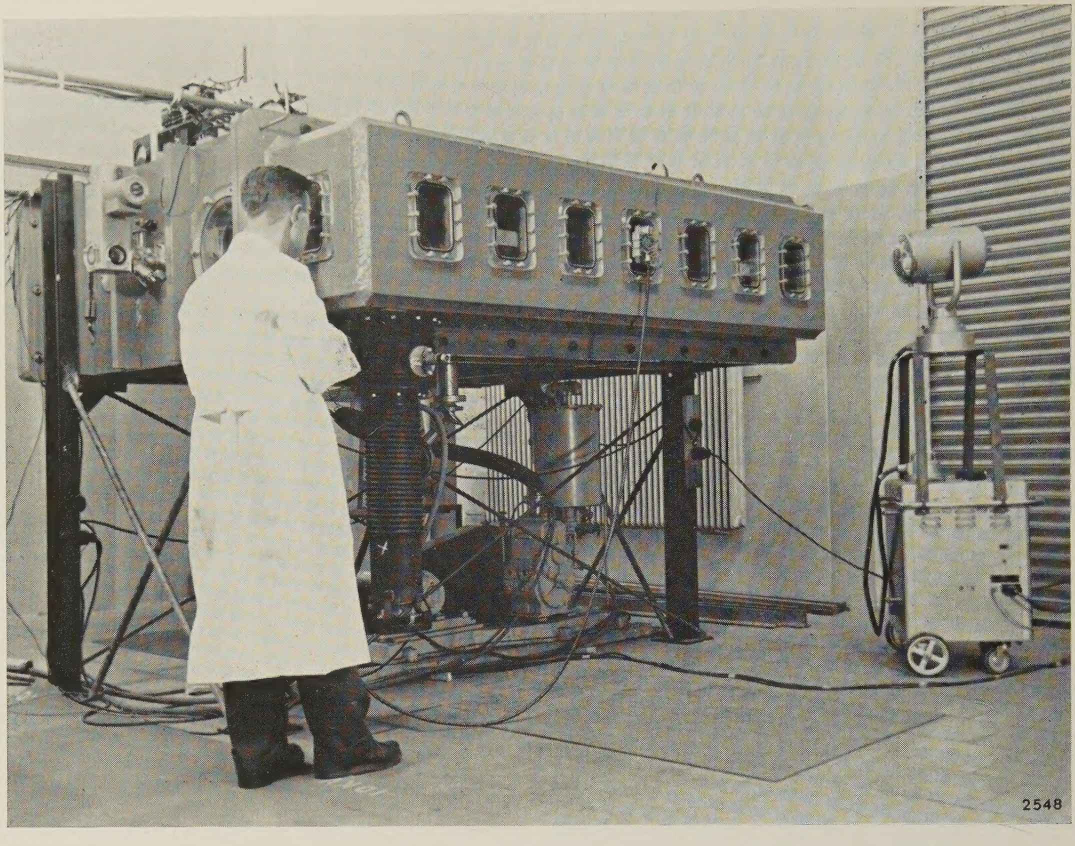

Fig. 27. Proving the modulator at Eindhoven. The stub tank, with the tuning fork mounted inside it, is provisionally sealed with a vacuum-tight cover plate provided with observation windows at the side where the dee stem will later be connected. Right: stroboscope for observing the vibration of the tuning fork.

on more frequently, but why this is so is not entirely clear.

The modulator has now been in operation some three years. Since it was not originally known whether the tuning fork would be satisfactory, the CERN had also built for all eventualities a modulator using a rotating capacitor. No call has been made on this, however. The first tuning fork has far exceeded its estimated life; the second remains as a stand-by, so that a third has now been constructed.

Summary. The frequency of the accelerating voltage of the CERN synchrocyclotron swings periodically from 29 to 16.5 Mc/s. This frequency modulation is effected by a capacitor made to vibrate at 55 c/s, which was developed by the Philips Eindhoven laboratories in cooperation with the CERN. The capacitor consists of an aluminium "tuning fork" roughly 60 cm long and 2 metres wide, and a stator of the same width attached to the dee stem. The very large amplitude of vibration required of the tuning-fork blades (1.25 cm) gives rise, at a resonant frequency of 55 c/s, to bending stresses that approach the endurance limit. In this respect an adequate safety margin was achieved by giving each blade a profile in the shape of a truncated wedge (minimum fatigue life 10^9 vibrations). The tuning fork is set in vibration by an electromagnetic drive system with an auxiliary mass, whereby a rigid mounting is avoided. As a result, virtually no vibrations are transmitted to surrounding parts. The drive system is fed by an *RC* oscillator operating at 27.5 c/s and an amplifier which delivers an output current of such form that the driving force (magnetic attraction) is almost purely sinusoidal. The *RC* oscillator is synchronized by a feedback signal which the vibrating tuning fork itself produces by periodically reflecting a beam of light on to a photocell. The drive electromagnet consumes about 30 W. During preliminary trials in the synchrocyclotron, the drive power required was found to be much greater, due to eddy-current losses in the tuning-fork blades caused by an unexpectedly large horizontal component of the stray field from the cyclotron magnet. This component was largely compensated by means of a DC coil consisting of ten turns and carrying a current of 400 A. The tuning-fork blades can vibrate not only in the desired fundamental mode, whereby the lips remain straight and parallel to the stator, but also in unwanted higher modes of vibration (observable by means of Chladni figures). It was found that, owing to the RF heating of the tuning fork, the resonant frequency of one of these higher modes coincided with a multiple of 55 c/s, resulting in the excitation of this mode. The coincidence was eliminated by fitting a stiffening rib of specific dimensions to each blade (care being taken that no other coincidences then arose). The heat generated by the current in the tuning fork (approx. 250 W) is removed by cooling the foot with water; cooling by radiation — the only alternative, since the tuning fork is contained in a vacuum — would lead to excessive temperatures. Non-uniform cooling involves the danger of warping. This was experimentally investigated by simulating with the aid of heater strips the calculated temperature distribution expected, and then measuring the deformations. The "lips" of the tuning fork were found to remain straight within about 0.2 mm. The relative position of the tuning fork and stator and the amplitude of the lips must be accurately maintained. For this purpose, the stator is fitted with five feeler devices. These supply signals which, via a "translator" and relays, actuate suitable combinations of four servomotors to automatically adjust the amplitude and/or appropriately displace the three points of suspension.

The first of the tuning forks constructed has operated satisfactorily for about three years, and has amply exceeded its estimated life.